University of Nebraska - Lincoln
DigitalCommons@University of Nebraska - Lincoln

Civil Engineering Theses, Dissertations, and Student Research

Civil Engineering

Fall 12-1-2015

VISCOELASTIC, FATIGUE DAMAGE, AND PERMANENT DEFORMATION CHARACTERIZATION OF HIGH RAP BITUMINOUS MIXTURES USING FINE AGGREGATE MATRIX (FAM)

Hesamaddin Nabizadeh
University of Nebraska-Lincoln, hesam.nabizadeh@gmail.com

Follow this and additional works at: http://digitalcommons.unl.edu/civilengdiss

Part of the Geotechnical Engineering Commons

Nabizadeh, Hesamaddin, "VISCOELASTIC, FATIGUE DAMAGE, AND PERMANENT DEFORMATION CHARACTERIZATION OF HIGH RAP BITUMINOUS MIXTURES USING FINE AGGREGATE MATRIX (FAM)" (2015). *Civil Engineering Theses, Dissertations, and Student Research*. 83.
http://digitalcommons.unl.edu/civilengdiss/83

This Article is brought to you for free and open access by the Civil Engineering at DigitalCommons@University of Nebraska - Lincoln. It has been accepted for inclusion in Civil Engineering Theses, Dissertations, and Student Research by an authorized administrator of DigitalCommons@University of Nebraska - Lincoln.

www.manaraa.com

VISCOELASTIC, FATIGUE DAMAGE, AND PERMANENT DEFORMATION CHARACTERIZATION OF HIGH RAP BITUMINOUS MIXTURES USING FINE AGGREGATE MATRIX (FAM)

By

Hesamaddin Nabizadeh

A THESIS

Presented to the Faculty of

The Graduate College at the University of Nebraska

In Partial Fulfillment of Requirements

For the Degree of Master of Science

Major: Civil Engineering

Under the Supervision of

Professor Yong-Rak Kim

Lincoln, Nebraska

December, 2015

www.manaraa.com

VISCOELASTIC, FATIGUE DAMAGE, AND PERMANENT DEFORMATION CHARACTERIZATION OF HIGH RAP BITUMINOUS MIXTURES USING FINE AGGREGATE MATRIX (FAM)

Hesamaddin Nabizadeh, M.S.

University of Nebraska, 2015

Advisors: Yong-Rak Kim

Performance characteristics of bituminous mixtures play the most influential role in designing flexible pavement. These asphaltic mixtures can be considered as heterogeneous mixtures which composed of two primary components: fine aggregate matrix (FAM) phase and aggregate phase. The FAM phase acts as a critical phase in evaluating the performance characteristics including viscoelastic, fatigue damage, and permanent deformation characteristics of entire asphalt mixtures. This study evaluates the viscoelastic, fatigue damage and permanent deformation characteristics of bituminous mixtures containing 65% reclaimed asphalt pavement (RAP) by performing oscillatory torsional shear tests of cylindrical bars of FAM using a dynamic mechanical analyzer. Moreover, this study investigates a linkage between performance characteristics of asphalt concrete (AC) mixture and its corresponding FAM phase.

To meet the objectives of this study, laboratory tests were performed for several FAM mixtures with 65% reclaimed asphalt pavement and different types of rejuvenators and one warm mix asphalt (WMA) additive. Test results were then analyzed using viscoelastic theories and fatigue prediction models based on continuum damage

www.manaraa.com

mechanics. Furthermore, obtained laboratory test results were compared with corresponding test results of asphalt concrete mixtures. The test results indicated that rejuvenators change properties and performance behavior related to fatigue damage and permanent deformation of high reclaimed asphalt pavement mixtures. In addition, test results of FAM phase were generally linked well with asphalt concrete mixture test results, and they vividly depicted that FAM phase could provide core information to predict the behavior of the asphalt concrete mixture.

www.manaraa.com

To my parents,

Without whom none of my success would be possible

www.manaraa.com

ACKNOWLEDGMENTS

I would like to thank my supervisor, Dr. Yong-Rak Kim for his guidance during this study. Also, I would like to thank Dr. Maria Szerszen and Dr. Ruqiang Feng for serving as committee members.

I would like to thank Nebraska Department of Roads (NDOR) for their financial supports. Also, I would like to thank Hamzeh Haghshenas for sharing his experimental results (asphalt concrete mixture test results) with me, and letting me to use them in my thesis. My great appreciation to Amaris T. Baker for her help to revise my thesis.

My heartfelt appreciation to my parents, my sister, and my brothers for their love, encouragement, and support, and I would love to express my sincere gratitude to them. Their love, encouragement, and support were deeply significant to give me strength to complete this research.

www.manaraa.com

TABLE OF CONTENTS

www.manaraa.com

www.manaraa.com

www.manaraa.com

LIST OF FIGURES

www.manaraa.com

www.manaraa.com

www.manaraa.com

LIST OF TABLES

www.manaraa.com

1. CHAPTER ONE

INTRODUCTION

1.1. Overview

Bituminous mixtures have been commonly used in different simple and complex pavement construction including driveways, roadways, airport runways, and many more. It is vivid that a lot of money has to be spent on constructing and maintaining these construction annually, and one of the most effective parameters about construction and maintaining cost is materials used to make these construction. The United States annually spends billions of dollars to develop pavement construction such as roadways, highways, and also to maintain these construction. It can be directly inferred that bituminous mixtures play a significant role on the construction and maintenance. In addition, selecting the appropriate materials based on the importance, age (long term or short term), environmental conditions, and the application of the construction is a substantial factor to minimize the cost of the construction.

Nowadays, a number of researchers (Al-Qadi et al., 2012; Mogawer et al., 2012; Moghadas Nejad et al., 2014; Sondag et al., 2002; Zhou et al., 2014) studied to evaluate the use of reclaimed asphalt pavement (RAP) in constructing pavement by decreasing the percentage of virgin aggregates and virgin binder. Using the recycled materials is economically beneficial and it decreases the cost of the pavement construction; it also has environmental impact associated with extraction, transportation, processing of natural materials, and saving places for disposal of the recycled materials. Therefore, using the

www.manaraa.com

reclaimed asphalt pavement is economically and environmentally beneficial. However, the implementation of mixtures containing reclaimed asphalt pavement has undesired effects because of inherent characteristics of reclaimed asphalt pavement such as inconsistent aggregate properties and stiff (aged) asphalt binder. Consequently, towards arriving at an efficient use of reclaimed asphalt pavement, the properties of recycled asphalt pavement should be properly engineered.

A large number of research studies (Austerman et al., 2009; Goh and You, 2011; Im and Zhou, 2014; Mallick et al., 2008; Mogawer et al., 2009; Mogawer et al., 2013; Shen et al., 2007a; Shu et al., 2012) has been done to properly engineer and improve the properties of mixtures containing reclaimed asphalt pavement, and it was indicated that rejuvenating agents (Shen et al., 2007b; Tran et al., 2012; Yu et al., 2014; Zaumanis et al., 2014) and warm mix asphalt (WMA) additives (Tao and Mallick, 2009; Timm et al., 2011; Zhao et al., 2012; Zhao et al., 2013) can fairly improve the engineering properties of mixtures containing reclaimed asphalt pavement. These agents and additives can mitigate the effect of aged binder and make the mixture softer.

There are several different methods to characterize the performance characteristics of asphalt mixtures. The conventional and typical method to evaluate the properties of asphalt mixtures are performing experimental tests (e.g., dynamic modulus, flow number) on asphalt concrete (AC) mixtures. But, these tests are costly and time consuming; also expensive equipment and skilled personnel are required to fabricate and test asphalt concrete mixtures and specimens. Hence, it implies that a new method should be employed to overcome these shortcomings.

www.manaraa.com

Several researchers (Branco and Franco, 2009; Kim et al., 2002; Kim et al., 2003a; Kim and Little, 2005; Kim et al., 2003b; Kim et al., 2006; Li et al., 2015; Underwood and Kim, 2013; Vasconcelos et al., 2010) have tried to develop a new method of performing rheological tests using fine aggregate matrix (FAM) samples to determine the performance characteristics of asphalt mixtures. In this method, instead of performing tests on asphalt concrete mixtures, aggregates retained on sieve No. 16 are excluded from asphalt concrete mixtures and tests are conducted on the obtained mixture. The FAM phase thus consists of asphalt binder, fine aggregates, fillers, and air voids, and this phase plays a significant role in estimating the damage and deformation of entire asphalt concrete mixtures. A successfully developed testing protocol using FAM has the potential to result in specification-type test methods because of efficiency, simplicity, and repeatability.

1.2. Research Objectives

The primary objective of this study is to examine the effects of different types of rejuvenating agents and warm mix asphalt additive on performance characteristics of asphaltic mixtures containing high-percentage (65% in this study) reclaimed asphalt pavement using FAM tests. Also, this study explores a linkage in the performance characteristics between asphalt concrete mixture and its corresponding FAM phase.

1.3. Research Methodology

Figure 1.1 illustrates the research methodology employed to do this study. A dynamic mechanical analyzer, AR2000ex Rheometer, was employed to perform different types of torsional shear tests on FAM specimens including strain sweep test, frequency sweep test, time sweep test, and creep-recovery test. Initially, strain sweep tests were performed to

www.manaraa.com

determine the linear viscoelastic (LVE) region in terms of homogeneity concept. Subsequently, frequency sweep tests were conducted to evaluate static relaxation behavior of FAM using the level of strain within linear viscoelastic region obtained from the strain sweep tests. Then, time sweep tests were carried out to evaluate the fatigue resistance of mixtures using strain levels that were high enough to create fatigue cracks in specimens. Finally, creep-recovery tests were conducted to evaluate the permanent deformation characteristics of FAM mixtures.

www.manaraa.com

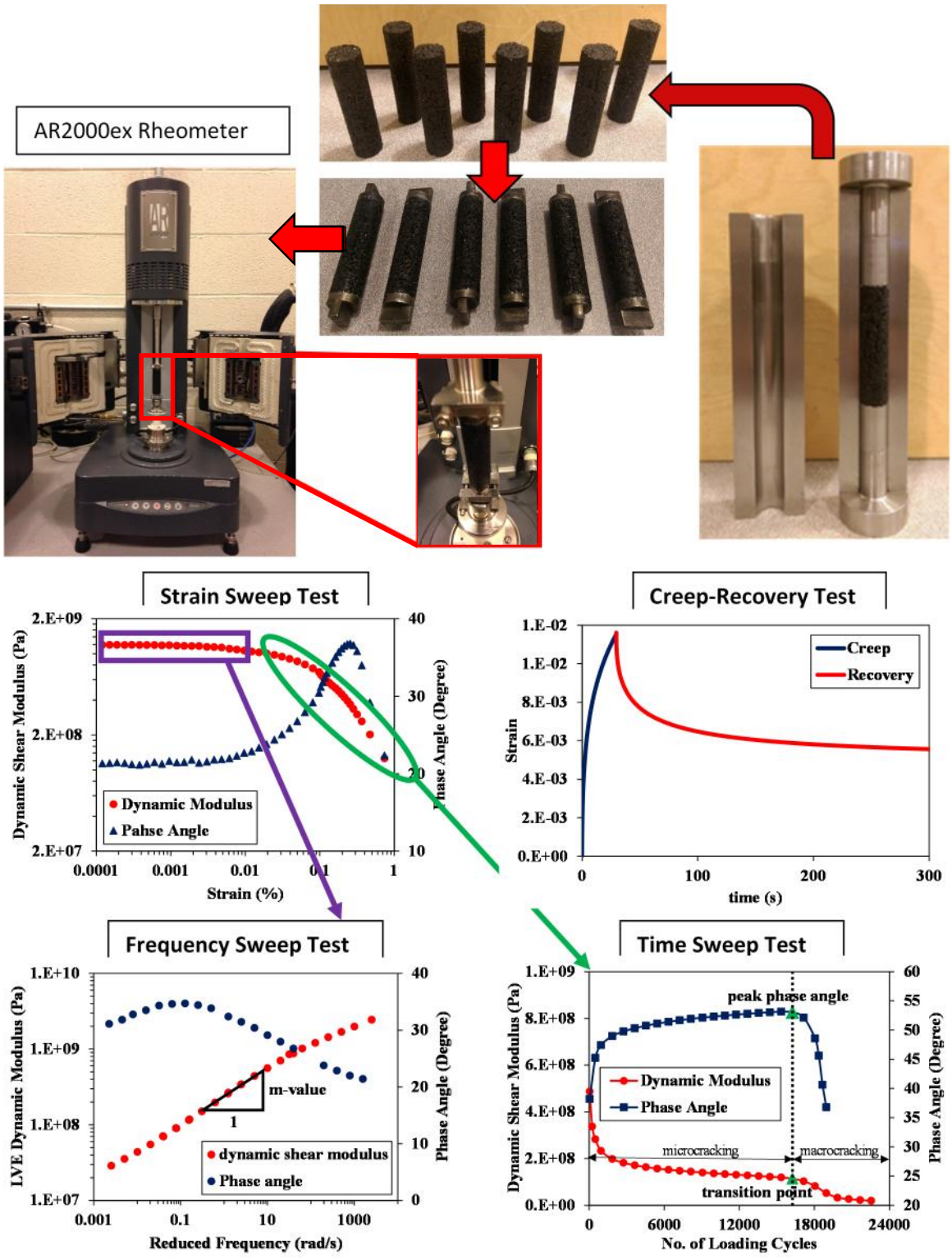

Figure 1.1. Research methodology used in this study.

www.manaraa.com

2. CHAPTER TWO

LITERATURE REVIEW

2.1. Fine Aggregate Matrix (FAM)

An asphalt concrete mixture is composed of coarse aggregates and a matrix phase, and the matrix phase is considered herein a separate phase containing asphalt binder, fine aggregates passing sieve No. 16 (mesh size of 1.18 mm), and entrained air voids. The matrix phase has been called FAM in numerous research studies (Branco and Franco, 2009; Im et al., 2015; Karki, 2010; Karki et al., 2015; Kim and Aragão, 2013; Kim et al., 2002; Kim and Little, 2005; Kim et al., 2003b; Kim et al., 2006; Palvadi et al., 2012; Underwood and Kim, 2013; Vasconcelos et al., 2010). A microstructure of asphalt concrete is illustrated in Figure 2.1, and coarse aggregates and FAM phase can easily be seen in the figure.

FAM plays a substantial role on the performance characteristics (e.g., viscoelastic and viscoplastic properties, fatigue resistance) of asphalt mixtures, and the quality of FAM considerably affects the mechanical characteristics of the entire asphalt concrete mixture. Several studies have been conducted to develop a specification-type testing methodology using FAM to predict the behavior of the entire asphalt mixture (Im, 2012; Im et al., 2015; Karki, 2010; Karki et al., 2015; Kim and Aragão, 2013; Li et al., 2015; Underwood and Kim, 2012; Underwood and Kim, 2013).

www.manaraa.com

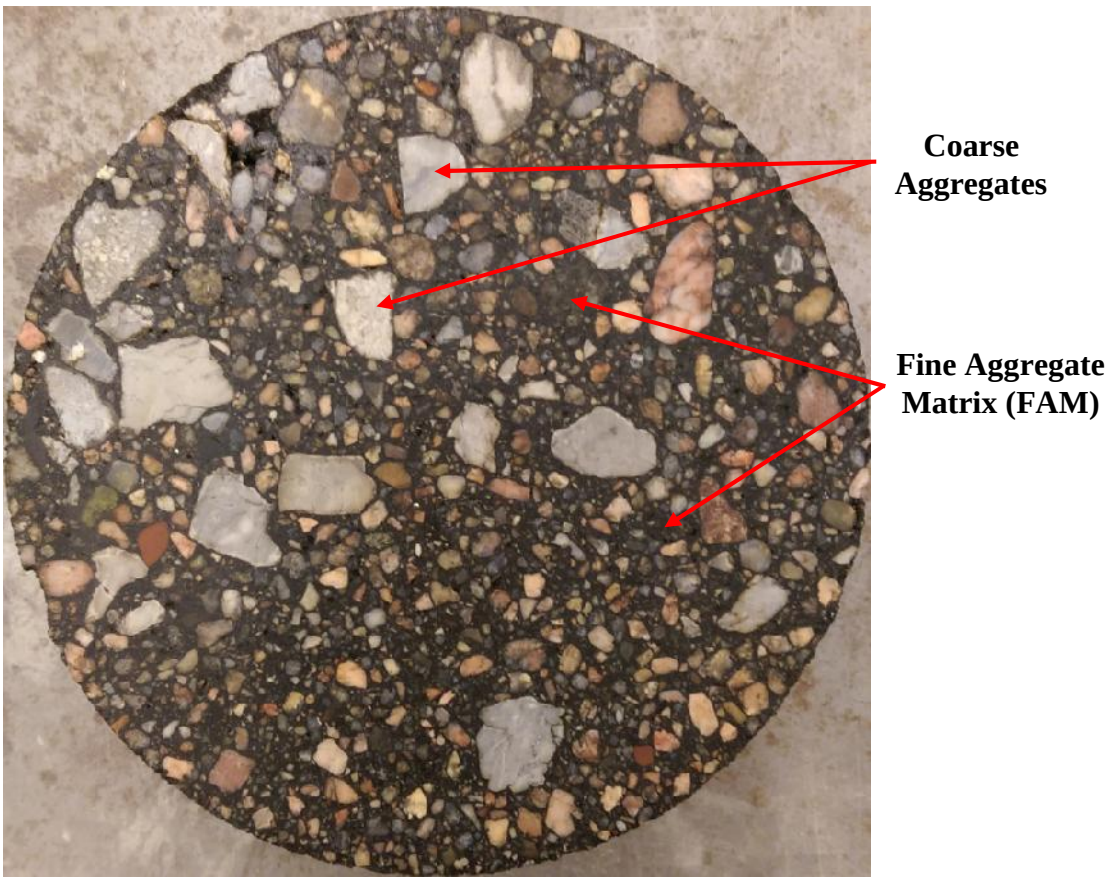

Figure 2.1. Asphalt concrete microstructure with two phases: coarse aggregates and fine aggregate matrix.

Kim and Little (2005) explored a test to evaluate the effect of fine aggregates and mineral fillers on the fatigue damage. They made small cylindrical sand asphalt samples (12 mm diameter, 50 mm long) using mastics, pure binders, and modified binders. Different dynamic mechanical tests in a strain-controlled mode (i.e., strain sweep test, frequency sweep test, and time sweep test) were performed using a dynamic mechanical analyzer. They performed frequency sweep tests to determine viscoelastic properties of sand asphalt samples and evaluated fatigue resistance of mixtures by conducting time

www.manaraa.com

sweep tests. They found sand asphalt samples could successfully characterize basic material properties and fatigue damage performance of binders and mastics.

Branco (2009) tried to develop a new methodology to evaluate fatigue cracking of the FAM phase of asphalt mixtures using a dynamic mechanical analyzer. To that end, two methods were employed: 1) computing the energy dissipated in viscoelastic deformation, permanent deformation, and fracture, 2) applying a constitutive relationship to model nonlinear viscoelastic response and damage under cyclic loading. Then, small FAM specimens were fabricated, and different types of torsional shear tests (e.g., strain sweep, time sweep) were performed. Finally, she could develop two new methods to evaluate fatigue damage in asphalt mixture independent of the mode of loading.

Vasconcelos et al. (2010) experimentally evaluated the diffusion of water in different FAM mixtures using gravimetric sorption measurement. They regarded FAM as a representative homogenous volume of hot mix asphalt. Two aggregate types (i.e., Basalt and Granite) and three asphalt binders (i.e., PG 58-22, PG 58-28, and PG 58-10) were selected to make FAM specimens; by doing experimental tests, it was inferred that FAM could successfully estimate water diffusion.

Karki (2010) used a computational micromechanics model to estimate the dynamic modulus of asphalt concrete mixtures using the properties of the constituents in the heterogeneous microstructure. The model considered the asphalt concrete mixtures as two different components: the viscoelastic FAM and the elastic aggregate phase. He made the Superpave gyratory compacted FAM to represent the FAM phase placed in its corresponding asphalt concrete mixture. Then, he tried to determine the mechanical

www.manaraa.com

properties of asphalt concrete mixture and its corresponding FAM phase. Dynamic modulus tests were then conducted on asphalt concrete samples to measure the dynamic modulus of mixtures, and torsional strain frequency sweep tests were performed on FAM samples to determine the dynamic modulus of FAM samples. He found out that the results of FAM could reliably estimate the results of asphalt concrete mixture, and FAM could practically predict the behavior of the entire asphalt concrete mixture.

Im (2012) tried to understand the relation between mechanical characteristics (i.e., linear viscoelastic, nonlinear viscoelastic, and fracture properties) of asphaltic materials in mixture scale and component scale. To evaluate the mechanical characteristics of asphaltic materials in mixture scale, asphalt concrete samples were made; and FAM samples were fabricated to estimate the mechanical properties of asphaltic materials in component scale. Linear viscoelastic properties of asphalt concrete and its corresponding FAM phase were evaluated by performing dynamic modulus and frequency sweep tests on asphalt concrete and FAM samples, respectively. Additionally, viscoelastic properties of asphalt concrete mixtures and FAM were characterized by conducting creep-recovery tests at different stress levels. He reported that FAM results could reasonably estimate asphalt concrete mixture results; therefore, FAM could predict the mechanical characteristics of the entire asphalt concrete mixture.

Underwood and Kim (2013) performed an experimental study to determine the suitable composition of materials to use in multiscale modeling and experimentation. It was assumed that asphalt concrete is composed of a four-scale assemblage of components with different characteristic length scales; binder, mastic, FAM, and asphalt concrete. A

www.manaraa.com

series of direct microstructural experiments were performed. Figure 2.2 illustrates dynamic modulus versus frequency in four different length scales (i.e., binder, mastic, FAM, and asphalt concrete mixture).

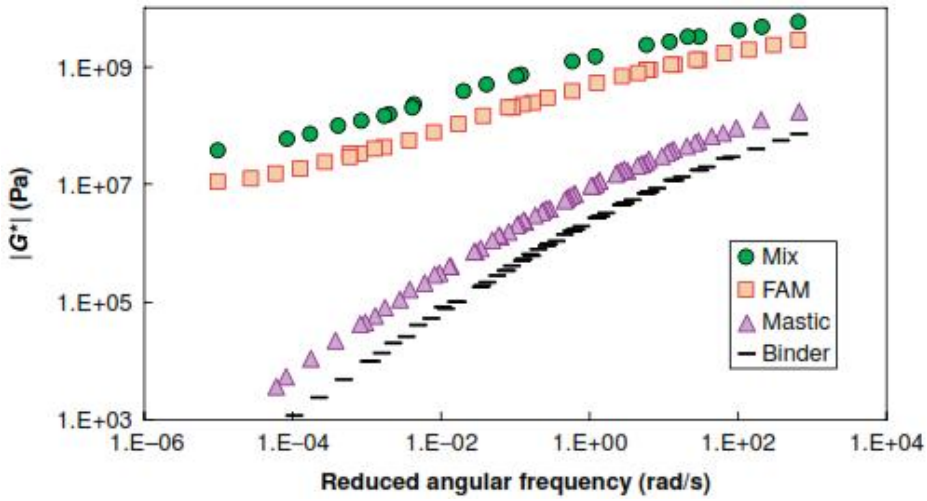

Figure 2.2. Dynamic modulus versus frequency in four different scales (Underwood and Kim, 2013).

Im et al. (2015) found a linkage in the deformation characteristics between an asphalt concrete mixture and its corresponding FAM phase. A simple test procedure was designed and a simple creep-recovery test was conducted at various stress levels on an asphalt concrete mixture and its corresponding FAM. The obtained test results of both mixtures (i.e., asphalt concrete mixture and FAM) were compared and analyzed using Schapery's single integral viscoelastic theory and Perzyna-type viscoplasticity with a generalized Drucker-Prager yield surface. They reported that there was a definite link between the asphalt concrete mixture and FAM in linear and nonlinear viscoelastic and viscoplastic deformation characteristics, and FAM could successfully predict the

www.manaraa.com

viscoelastic stiffness properties and viscoplastic hardening of asphalt concrete mixtures. Figure 2.3 depicted the linear viscoelastic creep compliance curves for the asphalt concrete mixture and its corresponding FAM phase before and after dimensionless process. The figure fully illustrated that results of the asphalt concrete mixture and FAM testing after the dimensionless process were approximately same.

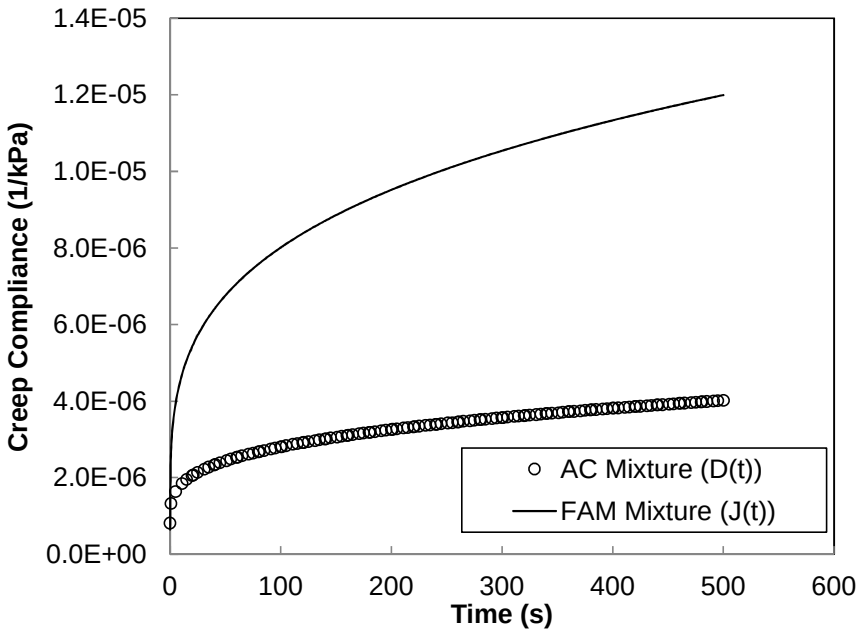

(a) before taking dimensionless process

www.manaraa.com

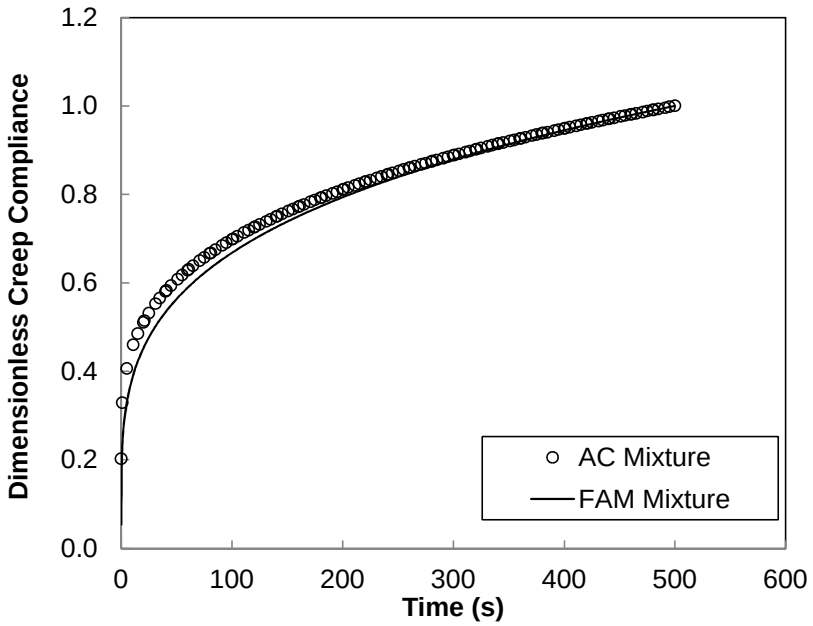

(b) after taking dimensionless process

Figure 2.3. Comparison of linear viscoelastic creep compliance curves (Im et al., 2015).

2.2. Reclaimed Asphalt Pavement (RAP)

Environmental conservancy is entitled as one of the most important considerations of the United States Department of Transportation strategic plan. To this end, Federal Highway Administration encourages the use of reclaimed asphalt pavement (RAP) to construct highway, in order to preserve the natural environment and reduce waste. In the United States, 80% of RAP annually removed from roadways is reused (Kandhal and Mallick, 1998). Many studies have been done to evaluate the effect of RAP on asphalt mixtures (Al-Qadi et al., 2012; Mogawer et al., 2012; Moghadas Nejad et al., 2014; Sondag et al., 2002; Zhou et al., 2014).

www.manaraa.com

Sondag et al. (2002) investigated the performance of the RAP, and they used resilient modulus and complex modulus testing to compare a mixture containing only virgin materials with mixtures containing varying amounts of RAP. 18 different mixtures were designed and made using two sources of RAP, varying amounts of RAP, and three different asphalt binders. Complex modulus tests were performed to evaluate the viscous and elastic properties of mixtures. Finally, it was reported that RAP made the mixture stiffer by increasing the resilient modulus and complex modulus, and decreased the viscous mixture properties and increased the elastic properties by decreasing the mixture phase angle.

Al-Qadi et al. (2012) performed a research to investigate the performance of high RAP hot mix asphalt and to find out considerations to utilize these high RAP content. They designed and made a control mixture with 0% RAP, and three hot mix asphalt mixtures with 30%, 40%, and 50% RAP, and they performed semicircular bending, beam fatigue, wheel tracking, complex modulus, moisture susceptibility, and flow number tests on hot mix asphalt (HMA) mixtures. It was observed that hot mix asphalt mixtures containing RAP showed equal or better performance than mixtures containing only virgin aggregate, and hot mix asphalt mixtures with high percentage of RAP (up to 50%) could be designed with proper volumetric characteristics.

Mogawer et al. (2012) characterized the performance characteristics of plant produced high RAP mixtures. Mixtures were collected from 18 plants in the Northeast part of the United States (i.e., New York, Vermont, and New Hampshire). Mixtures had varying amounts of RAP from 0% to 40%. They could evaluate rutting, cracking, stiffness,

www.manaraa.com

moisture susceptibility, and workability of different mixtures. It was reported that the cracking resistance decreased as the amount of RAP increased, and the stiffness of mixtures increased as the amount of RAP increased. In addition, the moisture damage and rutting resistance increased as the amount of RAP increased.

Zhou et al. (2014) performed a literature review to understand the performance of RAP and recycled asphalt shingles (RAS). Initially, it was indicated that the use of RAP could protect our environment, preserve energy, and considerably decrease the initial cost of asphalt mixtures. Then, the variability and the durability of RAP mixes were discussed with two main concerns. Based on the study in Texas, it was indicated that RAP had acceptable variability; finally, it was reported that dense graded RAP mixes could show similar or better performance than virgin mixes and RAP mixes showed poor cracking resistance, but better rutting resistance.

2.3. Rejuvenator

Rejuvenator is a recycling agent that has been typically used to improve properties of aged (stiff) binder, and suitable for highly oxidized or high RAP mixtures (Shen et al., 2007b). A number of research studies have been done using rejuvenators and indicate that rejuvenators have been efficiently used to increase the performance characteristics of asphalt mixtures containing high RAP (Im and Zhou, 2014; Mogawer et al., 2013; Shen et al., 2007a; Shen et al., 2007b; Tran et al., 2012; Yu et al., 2014; Zaumanis et al., 2014).

Tran et al. (2012) evaluated the effect of a rejuvenated asphalt binder on performance properties of recycled binders and hot mix asphalt mixtures containing high RAP and RAS. The rejuvenator (Cyclogen L) was added directly to the virgin binder,

www.manaraa.com

which was selected as PG 67-22. Also, 0.5% liquid anti strip agent by weight of the virgin binder was added to the virgin binder. Three different mixtures were designed and fabricated including a virgin mixture (control mixture), control mixture with 50% RAP, and control mixture with 20% RAP plus 5% RAS. Three different tests (i.e., tensile strength ratio, asphalt pavement analyzer, and dynamic modulus) were carried out on mixtures. It was reported that the use of rejuvenator slightly improved moisture resistance, and made mixture softer. In addition, mixtures could meet rutting failure criteria.

Mogawer et al. (2013) assessed the effects of rejuvenators on the stiffness of mixtures containing high RAP and RAS. They evaluated if rejuvenators could help an aged binder (i.e., RAP or RAS binder) combined with virgin binder. To that end, three different rejuvenators were selected and added to a virgin binder (i.e., PG 58-28) at a dosage recommended by manufacturers. Four different mixtures were designed as control mixture, control mixture with 35% RAP plus 5% RAS, control mixture with 5% RAS, and control mixture with 40% RAP. Different experimental tests (i.e., dynamic modulus, rutting, moisture susceptibility, and reflective cracking) were performed on four mixtures; finally, it was reported that rejuvenators can decrease the stiffness of the aged binder, and the cracking resistance of rejuvenated mixtures improved, while, moisture susceptibility and rutting were undesirably impacted at the testing condition and the dosage used.

Zaumanis et al. (2014) performed an experimental study to evaluate effects of different recycling agents for renovating performance of 100% recycled asphalt and an aged asphalt binder. Six different recycling agents (i.e., waste vegetable oil, waste vegetable grease, organic oil, distilled tall oil, aromatic extract, and waste engine oil) were

www.manaraa.com

added to a virgin binder (i.e., PG 64-22). 100% RAP mixtures using different recycling agents were designed and fabricated, and different experimental tests (i.e., Hamburg wheel test, creep compliance, and tensile strength) were conducted on mixtures. It was concluded that the workability of the binder and mixtures was enhanced using recycling agents, and all rejuvenated mixtures were highly rut resistant. Also, all recycling agents improved low temperature performance of RAP, which was confirmed with creep compliance measurements at -10˚C.

2.4. Warm Mix Asphalt (WMA) Additive

Warm mix asphalt (WMA) is called as a generic term of technologies that allow producers of hot mix asphalt materials to decrease mixing and compaction temperatures 50˚F to 100˚F. Reducing plant mixing temperature causes fuel cost saving to the contractor. Also, reducing mixing and compaction temperatures results in decreasing any visible or invisible emissions that may cause health issues, odors, or greenhouse gases (Lange and Stroup-Gardiner, 2002). A lot of research studies have been done to evaluate the effect of WMA additives on the performance characteristics of asphalt mixtures containing RAP (Austerman et al., 2009; Goh and You, 2011; Mallick et al., 2008; Mogawer et al., 2009; Shu et al., 2012; Tao and Mallick, 2009; Timm et al., 2011; Zhao et al., 2012; Zhao et al., 2013).

Goh and You (2011) characterized the mechanical properties of porous asphalt mixtures containing one WMA additive and RAP. Four different mixtures were designed, fabricated, and tested including control mixture which was a conventional porous asphalt mixture, porous asphalt mixture containing 15% RAP, porous asphalt mixture with one

www.manaraa.com

WMA additive, and porous asphalt mixture containing 15% RAP and one WMA additive. They evaluated indirect tensile strength, permeability, dynamic modulus, and compaction energy index. They pointed out that compaction energy required for the control mixture (hot mix asphalt) was higher than the warm mixture containing 0.25% WMA additive. Also, the results of dynamic modulus clearly depicted that the control mixture had significantly higher values than the WMA mixture. In addition, the WMA mixture containing RAP showed the highest tensile strength between all mixtures.

Shu et al. (2012) conducted an experimental study to evaluate the moisture susceptibility of plant produced foamed WMA containing high RAP in Tennessee. Six different mixtures were made including hot mix asphalt containing 0% (control mixture) and 30% RAP, and WMA containing 0%, 30%, 40%, and 50% RAP, and different laboratory tests were carried out including moisture conditioning, tensile strength ratio, dynamic modulus, Superpave indirect tension, asphalt pavement analyzer, and Hamburg wheel tracking. It was concluded that the hot mix asphalt and plant produced foamed WMA mixtures exhibited almost similar moisture susceptibility.

Zhao et al. (2013) evaluated performance characteristics of WMA containing high RAP using laboratory performance tests. They evaluated fifteen control hot mix asphalt and WMA mixtures containing RAP ranging from 0% to 40%. Different laboratory tests were performed on mixtures including tensile strength ratio, flow number, asphalt pavement analyzer rutting, Hamburg wheel tracking, resilient modulus ratio, dissipated creep strain energy method from Superpave indirect tests, 50% stiffness reduction method and plateau value method from beam fatigue tests. It was reported that WMA-high RAP

www.manaraa.com

mixtures had more moisture and rutting resistance than WMA-low RAP mixtures, and less rutting and moisture resistance than hot mix asphalt-high RAP mixtures. However, WMA-high RAP showed more fatigue resistance than WMA-low RAP and hot mix asphalt-high RAP mixtures.

www.manaraa.com

3. CHAPTER THREE

MATERIALS AND SAMPLE FABRICATION

3.1. Materials

3.1.1. Aggregates

Aggregates passing sieve No. 16 were selected to make FAM, and 1.18 mm (sieve No. 16) aggregates were considered as the maximum aggregate size (MAS) in FAM. For this study, FAM gradation was obtained from an original asphalt concrete mixture gradation by excluding aggregates larger than 1.18 mm. Table 3.1 shows aggregate gradation for the original asphalt concrete mixture and Table 3.2 presents its corresponding FAM gradation. It should be noted that only one source of virgin aggregate (3ACR Gravel) was used to make FAM, because 3ACR gravel was the dominant virgin aggregate in the asphalt concrete mixture. Also, 0.45-power gradation curves of the original asphalt concrete mixture and its FAM are shown in Figure 3.1.

www.manaraa.com

Table 3.1. Gradation chart for virgin aggregates and reclaimed asphalt pavement.

Material	% Agg.	Aggregate Gradation (% Passing on Each Sieve)								
		19mm	12.5mm	9.5mm	#4	#8	#16	#30	#50	#200
RC 1	11	100	50	45	43	30	20	2.7	2.5	2.1
3 A Cr. Gravel	17	100	100	100	98	80	39.5	24.2	14.6	5.9
2A Gravel	7	100	100	100	95	6.8	2.5	0	0	0
RAP	65	100	95.8	91.3	75	54.1	38.9	28.7	19.9	8.6
Combined		100	91.8	88.3	76.8	52.5	34.3	23.1	15.7	6.8

Table 3.2. Gradation chart for fine aggregate matrix phase.

Material	% Agg.	Aggregate Gradation (% Passing on Each Sieve)				
		#16	#30	#50	#200	Pan
3 A Cr. Gravel	35	100	24.2	14.6	5.9	0
RAP	65	100	28.7	19.9	8.6	0
Combined		100	27.1	18.0	7.7	0

www.manaraa.com

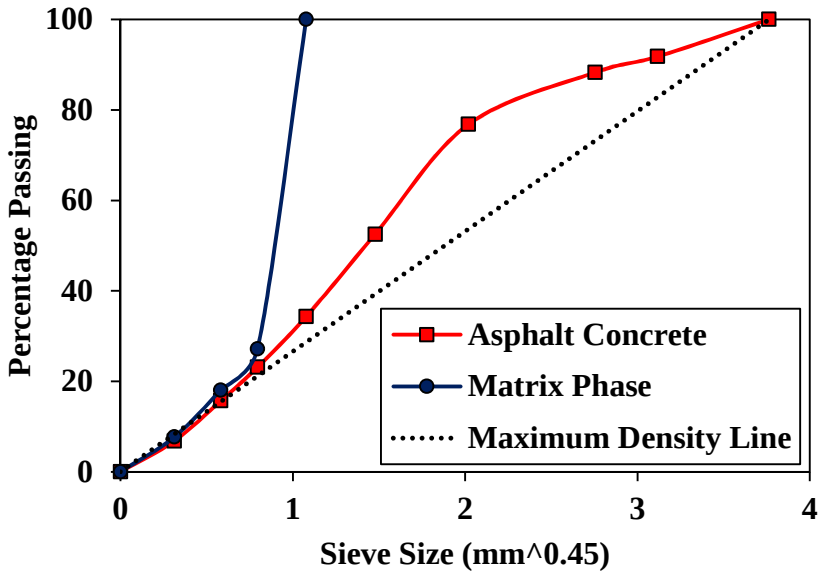

Figure 3.1. Virgin aggregate gradation curves: mixture and its fine aggregate matrix phase.

3.1.2. Reclaimed Asphalt Pavement (RAP)

One source of RAP passing sieve No. 16 was selected to make FAM mixtures. RAP gradation was obtained from the original asphalt concrete mixture gradation by excluding particles larger than 1.18 mm. Table 3.2 shows RAP gradation for FAM phase. Since RAP includes old binder as well as aggregates, the percentage of RAP binder needs to be identified to use the RAP appropriately in the FAM mixture design. To determine the percentage of RAP binder, three ignition tests were performed on RAP passing sieve No. 16, and at each test 1,700 grams of RAP was used. The percentage of RAP binder was determined at 9.34% based on weight of RAP. Before doing the ignition tests, RAP was dried out at room temperature for 24 hours.

www.manaraa.com

3.1.3. Binder

A Superpave performance graded PG 64-34 from Jebro Inc. was used to make mixtures. The binder was provided by Nebraska Department of Roads (NDOR).

3.1.4. Rejuvenators

Three rejuvenators, based on different production technologies (i.e., agriculture tech, green tech, and petroleum tech) were used. Different amounts for each rejuvenator were used based on the manufacture's suggestion as presented in Table 3.3. It should be noted that agriculture tech and petroleum tech rejuvenators were added to the virgin binder, while the green tech rejuvenator was directly added to the RAP.

Table 3.3. Amount of rejuvenators in the mixture

Rejuvenator	Amount of rejuvenator based on total weight of binder (%)
Agriculture tech	1.5
Green tech	7.8
Petroleum tech	6.2

3.1.5. Warm Mix Asphalt Additive

One amine-based WMA additive was selected in this study. The 0.292% WMA additive by the weight of virgin binder was directly added to the virgin binder.

3.2. FAM Mixture Design

The mixture design of FAM was conducted by using 65% RAP aggregate and 35% virgin aggregate based on Table 3.2. The process of the mixture design also included calculating the binder content which was based on the RAP binder content.

www.manaraa.com

The most challenging part of mixture design was to determine the proper amount of binder to make FAM. To this end, a rational assumption was made: the ratio of RAP aggregate to virgin aggregate is equal to the weight ratio of RAP binder to virgin binder as illustrated in Eq.3.1

$$W_{vb} = \frac{P_{va}}{P_{ra}} \times W_{rb} \qquad \textbf{Eq.3.1}$$

where W_{vb} = weight of virgin binder,

W_{rb} = weight of RAP binder,

P_{va} = percentage of virgin aggregate, and

P_{ra} = percentage of RAP aggregate.

As mentioned earlier, 65% RAP aggregate and 35% virgin aggregate were used to make the FAM. The percentage of old binder in the RAP mixture passing sieve No.16 was measured as 9.34% by weight of RAP through an ignition oven test. Based on the assumption and test results, weight of virgin binder could easily be calculated. For example, if the mixture contains 260 grams RAP aggregate (65%) and 140 grams virgin aggregate (35%), the weight of virgin binder would be 14.42 grams, since RAP contains 9.34% old binder. This results in the weight of RAP being 286.79 grams and the weight of old binder being 26.79 grams in the mixture. Additionally, it should be noted that the percentage of virgin binder was also 9.34% by the weight of virgin aggregate passing sieve No. 16.

www.manaraa.com

After determining the amount of virgin binder to be added in the FAM, the compaction density of FAM specimens should be determined. The compaction density of the FAM is defined as the ratio of mass of a FAM specimen to its volume as follows:

$$\circ_{FAM} = \frac{M_{FAM}}{V_{FAM}} \qquad \textbf{Eq. 3.2}$$

where M_{FAM} = mass of FAM,

V_{FAM} = volume of FAM, and

$\circ_{FAM}$ = density of FAM.

The bulk volume of each FAM specimen was calculated as 5.654 cm^3; it will be explained in section 3.4. Also, the compaction density of the FAM specimen was determined as 2.122 gr/cm^3 based on the volumetric design of FAM phase of the asphalt concrete specimen. By knowing the compaction density and the volume of each FAM specimen, weight of each specimen was easily obtained using Eq. 3.2.

3.3. FAM Mixtures Evaluated

Five FAM mixtures were prepared for this study by varying blending of aggregates, rejuvenators, and WMA additive. The five mixtures are listed in Table 3.4. As shown in the table, mixture C is the control mixture, and others are FAM mixtures with three different rejuvenators and the WMA additive.

www.manaraa.com

Table 3.4. Fine Aggregate Matrix Prepared.

Mixture	Asphalt Binder	Aggregates	Additive	Amount of additive
C	PG 64-34	Virgin aggregates (35%) RAP aggregates (65%)	-	-
CR1			Petroleum tech	6.2%
CR2			Green tech	7.8%
CR3			Agriculture tech	1.5%
CRW1			Petroleum tech rejuvenator, WMA	6.2% 0.292%

3.4. FAM Specimen Fabrication

This section describes the specific procedure implemented for FAM specimen fabrication. First, the virgin aggregates, RAP and the binder were preheated at a pre-determined mixing temperature for 75 minutes and thoroughly mixed with each other. The mixing temperature was determined at 160˚C for all mixtures except CRW1, which was considered as 138˚C to see the effect of WMA additive. The mixing process was conducted manually, since the amount of materials were small (approximately 500 grams). Second, the required amount of mixture to make each FAM specimen was heated up at a pre-determined compaction temperature for 30 minutes. The compaction temperature was set at 138˚C for others except the CRW1, set at 124˚C. In the next step, the loose FAM mixture was evenly distributed in a specially designed and fabricated mold and compacted manually. Next, the mold was put in a freezer at temperature -18˚C for 10 minutes to cool it down so as to facilitate specimen removal from the mold without undue distortion of specimens. Then, the specimen was removed from the mold and placed at a room temperature of 25˚C for 24 hours. Finally, epoxy glue was used to secure holders to the specimen to make specimens

www.manaraa.com

ready for testing. After gluing, the specimen was placed at the room temperature of 25˚C for 5 hours. These specimen fabrication steps are summarized in Table 3.5.

Table 3.5. Procedure to fabricate FAM specimen.

Steps	Temperature	Time
Pre-heating	160˚C and 138˚C	75 min
Mixing		
Heating	138˚C and 124˚C	30 min
Compacting		
Cooling	-18˚C	10 min
Equilibration	Room temperature	24 hours
Gluing		
Equilibration	Room temperature	5 hours

3.4.1. Compaction Mold

A cylindrical compaction mold was designed and fabricated for this study as shown in Figure 3.2. The dimensions of the mold are presented in Table 3.6. The inner surface of the mold was machined to make a very smooth surface on the specimen without any substantial flaw. Kim and Little (2005) mentioned that this treatment considerably helps obtain repeatable test results. The smooth surface was a critical feature in minimizing random behavior in terms of fatigue crack initiation and propagation in the torsional loading mode.

www.manaraa.com

(a) **(b)**

Figure 3.1. Compaction mold for FAM specimen (a) before assembly (b) after assembly.

Table 3.6. Compaction mold dimensions.

Material	Stainless steel
Length	130 mm
Inner diameter	12 mm
Outer diameter	30 mm
Thickness	9 mm

www.manaraa.com

3.4.2. FAM Specimen for Testing

FAM specimens compacted are in cylindrical shape as shown in Figure 3.2. The cylindrical sample geometrics were implemented in this study for easy data analysis and to prevent complex stress distributions. The specification of each FAM specimen is presented in Table 3.7. 12 grams of loose FAM mixture was determined using compaction density to make each compacted specimen, 50 mm long with a 12 mm diameter.

Figure 3.2. FAM specimens, 12 grams mass, 50 mm long with a 12 mm diameter.

www.manaraa.com

Table 3.7. FAM specimen specifications.

Height	50 mm
Diameter	12 mm
Weight	12 gr
Percentage of binder	9.34%
Weight of RAP aggregate	7.07 gr
Weight of RAP binder	0.73 gr
Weight of virgin aggregate	3.81 gr
Weight of virgin binder	0.39 gr
Specific density	2.122 gr/cm^3

For torsional testing, two fixtures were secured to both ends of each FAM specimen using epoxy glue. Gluing was done carefully not to cause any undesirable stress concentrations at both ends. Moreover, in gluing process, it was considered that fixtures should be inline. To this end, a small tool was designed and fabricated to make sure the two fixtures lined up. Figure 3.3 and Figure 3.4 illustrate the FAM specimens with fixtures glued and the tool to line up the fixtures.

Figure 3.3. Fine aggregate matrix specimens with holders.

www.manaraa.com

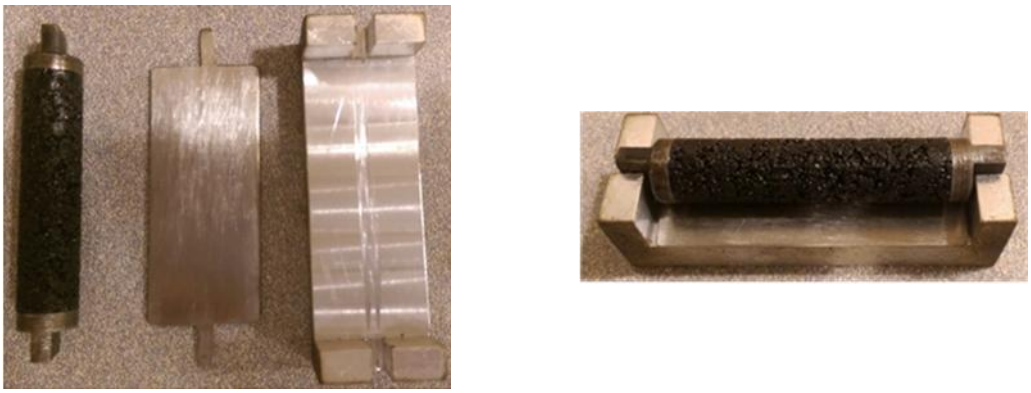

Figure 3.4. The tool to make holders inline.

www.manaraa.com

4. CHAPTER FOUR

LABORATORY TESTS AND RESULTS

This chapter describes different laboratory tests performed to characterize various different material behavior and present test results. Different torsional shear tests using a dynamic mechanical analyzer were performed on FAM specimens to evaluate fundamental properties and performance characteristics of different asphalt mixtures.

4.1. Dynamic Mechanical Analyzer Testing

Dynamic mechanical analysis (DMA) can be simply defined as analyzing the material's response to an applied oscillatory force to a specimen. In other words, dynamic mechanical analysis is a method to characterize materials' characterization as a function of frequency, temperature, stress, time or a combination of these parameters. A dynamic mechanical analyzer applies a sinusoidal stress (or strain) to a specimen, and it causes sinusoidal strain (or stress) as shown in Figure 4.1. By determining the lag between stress and strain sine waves and the maximum of the sine wave, parameters (e.g., modulus, viscosity, phase angle) can be obtained. It should be noted that tests can be performed in a controlled-stress or a controlled-strain mode (Menard, 2008).

www.manaraa.com

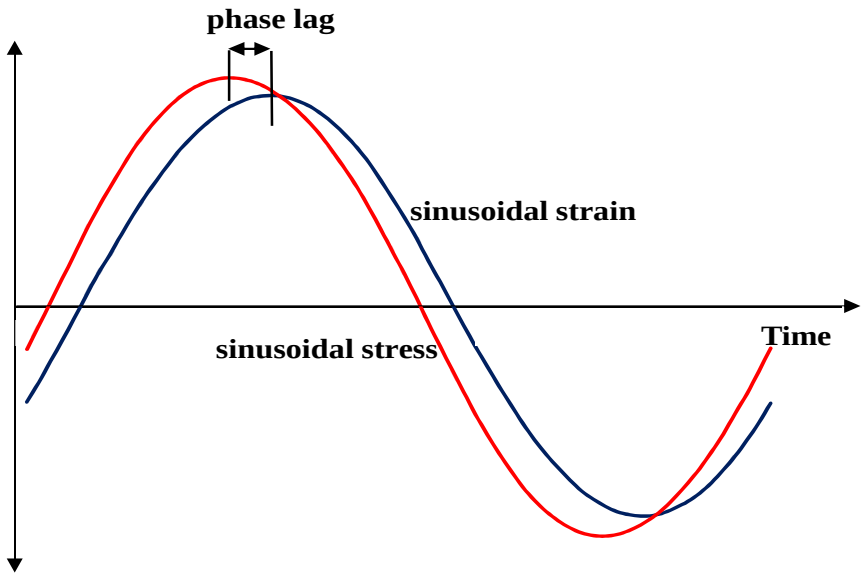

Figure 4.1. Applied sinusoidal stress to sinusoidal strain with the phase angle.

4.1.1. Testing Machine, AR2000ex Rheometer

In this study, a dynamic mechanical analyzer, AR2000ex rheometer, was employed to perform tests as shown in Figure 4.2. The machine had three main parts: a control computer, a testing station, and a system controller. The testing station is a main unit to conduct tests and it has an environmental chamber to control testing temperature. The environmental chamber is connected to a Nitrogen tank to control temperature from -160˚C to 200˚C.

www.manaraa.com

Figure 4.2. The dynamic mechanical analyzer, AR2000ex rheometer.

4.2. Laboratory Testing and Results

Three types of strain-controlled torsional oscillatory shear tests (i.e., strain sweep, frequency sweep, and time sweep) and static creep-recovery tests were performed on FAM specimens. First, strain sweep tests were conducted to determine linear viscoelastic region in terms of homogeneity concept and these tests also determined strain levels which produced maximum phase angles. Subsequently, frequency sweep tests were carried out to evaluate viscoelastic properties of each FAM mixture using strain levels within linear viscoelastic region. Then, using strain levels larger than strains that satisfy linear viscoelasticity, time sweep tests were performed to evaluate fatigue resistance potential. Finally, static creep-recovery tests were conducted to determine the amounts of creep strain and irrecoverable strain of individual FAM mixtures at different stress levels. Table 4.1 and Table 4.2 present testing details.

www.manaraa.com

Table 4.1. Strain-controlled torsional oscillatory shear tests.

Type of Test	Frequency (Hz)	Temperature (˚C)	Strain (%)	No. of Samples
Strain Sweep	0.1	40	0.0001 to 10	3
	10	25		3
	10	10		3
Frequency Sweep	0.1-10	10-20-30-40	0.001	3
Time Sweep	10	25	0.15, 0.30	3
			0.20, 0.35	3
			0.25, 0.40	3
Total Number of Samples				21

Table 4.2. Static creep-recovery test procedure.

Creep		Recovery		Temperature (˚C)	No. of Samples
Shear stress (Pa)	Time (sec)	Shear stress (Pa)	Time (sec)		
5	30	0	300	40	2
15	30	0	300	40	2
25	30	0	300	40	2
50	30	0	300	40	2
75	30	0	300	40	2

Each specimen was equilibrated for 30 minutes in the environmental chamber at the test temperature before doing the test to ensure that the inside temperature of the specimen in all areas was same as the desired temperature to perform the test.

www.manaraa.com

4.2.1. Torsional Shear Strain Sweep Test

Strain sweep tests were performed at different temperatures and frequencies, as presented in Table 4.1. Tests were started at 0.0001% strain and continued until specimen failure, and they were performed at three different frequency-temperature combinations; 0.1 Hz - 40˚C (compliant condition), 10 Hz - 10˚C (stiff condition), and 10 Hz - 25˚C.

The first two frequency-temperature combinations were conducted to determine the linear viscoelastic region based on the homogeneity concept for the entire frequency and temperature domain that frequency sweep tests were performed. Homogeneity concept clearly defined that the ratio of stress response to any applied strain was independent of strain magnitude. This concept could be considered for the strain sweep test by observing dynamic modulus as strain increases. Marasteanu and Anderson (2000) concluded that the linear viscoelastic region held until 10% drop in the initial value of the dynamic modulus. The third frequency-temperature combination (i.e. 10 Hz - 25˚C) was conducted specifically to carry out time sweep tests for determining strain levels that could produce maximum phase angle, because time sweep tests were conducted at 10 Hz and 25˚C.

The results of the strain sweep tests are illustrated in Figure 4.3. The results depict that the linear viscoelastic region held until around 0.01% strain, and the control mixture had the stiffest behavior at all testing temperatures. Additionally, the petroleum tech rejuvenated mixture showed the softest behavior between rejuvenated mixtures without the WMA additive. Since the petroleum tech rejuvenator showed the most softening effect on the mixture than other rejuvenators, the petroleum tech rejuvenator was selected to add to the binder with the WMA additive. This was to understand the effects of the rejuvenator

www.manaraa.com

and the WMA additive when mixing and compaction temperatures were decreased. The results depicted that the mixture containing the petroleum tech rejuvenator and the WMA additive showed softer behavior than the petroleum tech rejuvenated mixture even by decreasing mixing and compaction temperatures. Also, the green tech and the agriculture tech rejuvenated mixtures displayed nearly the same behavior.

Furthermore, linear viscoelastic dynamic shear moduli at three different test temperatures are presented in Table 4.3. It should be stated that strain sweep tests at a temperature of 10˚C were performed until approximately 0.3% strain, because at this temperature specimens showed a very stiff behavior. The machine had reached the maximum torque capacity and tests were ended at around 0.3% strain.

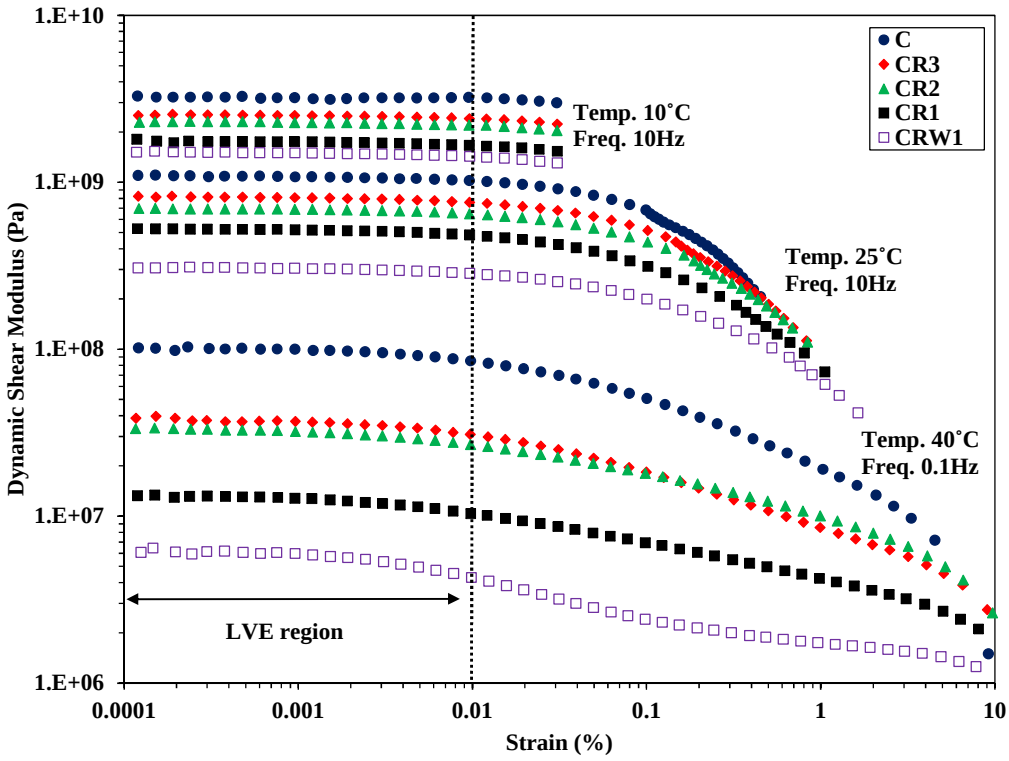

Figure 4.3. Torsional shear strain sweep test results at different frequency-temperature combinations.

www.manaraa.com

Table 4.3. Linear viscoelastic dynamic shear modulus (Pa) at three different test temperatures.

Mixture	Testing temperature (˚C)		
	10	25	40
C	3.22E+09	1.19E+09	1.02E+08
CR3	2.55E+09	8.66E+08	3.86E+07
CR2	2.31E+09	8.24E+08	3.34E+07
CR1	1.75E+09	5.27E+08	1.33E+07
CRW1	1.51E+09	3.07E+08	6.07E+06

4.2.2. Torsional Shear Frequency Sweep Test

Each frequency sweep test was performed by changing the loading frequency at a certain level of strain and temperature. In this study, frequency increased from 0.1 Hz to 10 Hz at each test to determine the effect of loading time on the stiffness of FAM, while the strain level was fixed at 0.001%. The strain level at 0.001% was low enough to prevent any non-linear behavior with and without damage. Also, each specimen was tested at four different test temperatures (i.e., 10˚C, 20˚C, 30˚C, and 40˚C) to observe the effect of temperature on the stiffness of FAM mixtures.

Typical results of the frequency sweep test performed on mixture CR2 are illustrated in Figure 4.4. The results presented that by increasing frequency, dynamic shear modulus increased, and by increasing temperature, dynamic shear modulus decreased. Also, Table 4.4 presents dynamic shear moduli for all mixtures at 10 Hz and all test temperatures. The results indicated that the control mixture had stiffer behavior than other mixtures, and the mixture containing the WMA additive and the petroleum tech rejuvenator had the softest behavior. Moreover, the petroleum tech rejuvenated mixture showed softer

www.manaraa.com

behavior than agriculture tech and green tech rejuvenated mixtures, which showed similar behavior. It should be noted that the main purpose of performing frequency sweep tests was to identify viscoelastic properties of the mixtures which is provided in the next chapter in detail.

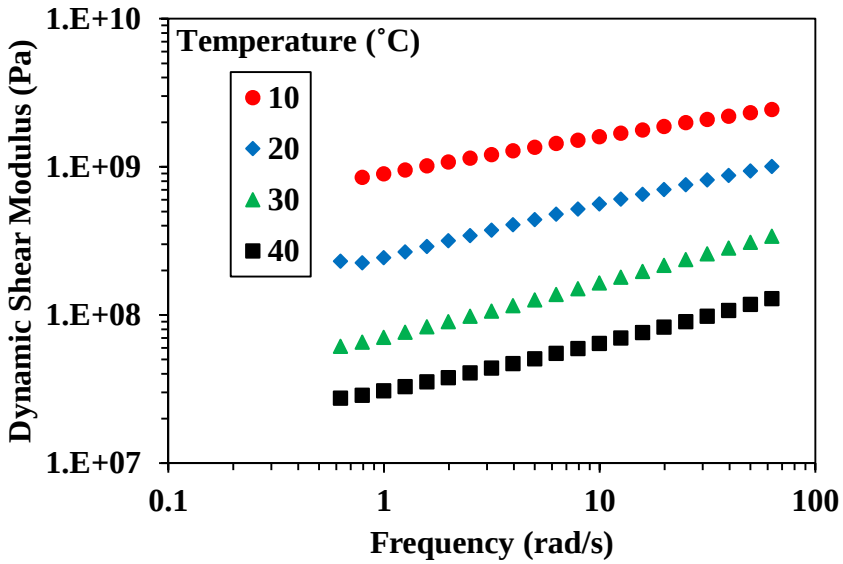

Figure 4.4. Results of the frequency sweep test at 0.001% strain on the mixture CR2.

Table 4.4. Dynamic shear modulus at 10 Hz and all test temperatures.

Mixture	Dynamic shear modulus (Pa)			
	10˚C	20˚C	30˚C	40˚C
C	3.10E+09	1.66E+09	8.26E+08	3.65E+08
CR3	2.58E+09	1.25E+09	5.53E+08	2.13E+08
CR2	2.59E+09	1.12E+09	4.09E+08	1.60E+08
CR1	1.77E+09	7.25E+08	2.77E+08	8.96E+07
CRW1	1.55E+09	5.36E+08	1.63E+08	5.24E+07

www.manaraa.com

4.2.3. Torsional Shear Time Sweep Test

Time sweep tests were carried out to determine fatigue resistance of different mixtures. Tests were performed at 10 Hz and 25˚C with three different strain levels, and they were continued until the specimen failure and macro-cracks could be seen in the specimen by the end of tests.

Since one of the main purposes of the time sweep tests was to create cracks in the specimens, strain levels were designated high enough to make cracks, and they were selected out of the linear viscoelastic region. Strain levels were selected based on two considerations: making fatigue cracks in the specimen at the end of the test, and finishing the test with reasonable amount of testing time. Thus, three strain levels; 0.15%, 0.20% and 0.25%; were selected for all mixtures except CRW1, which were tested with 0.30%, 0.35%, and 0.40% strains.

Typical results of time sweep tests performed on CR2 mixture at strain level of 0.25% are illustrated in Figure 4.5. As it can be distinctly seen in the figure and mentioned by researchers (Branco and Franco, 2009; Kim et al., 2002; Kim et al., 2003a; Kim and Little, 2005; Kim et al., 2003b), there were three stiffness reduction steps in the time sweep test results: rapid reduction in early step, constant rate of reduction, and accelerated degradation step. Also, there were two inflection points: first inflection point (P_f) and second inflection point (P_s). These inflection points showed microcracking and macrocracking propagation in the specimen and changing material's behavior. P_f indicated microcracking development in the specimen with decreasing rate of stiffness, and P_s represented macrocracking propagation in the specimen. There was another point between

www.manaraa.com

the two inflection points, called transition point (P_t). P_t implied shifting from microcracking to macrocracking, and at this point the rate of stiffness reduction increased drastically.

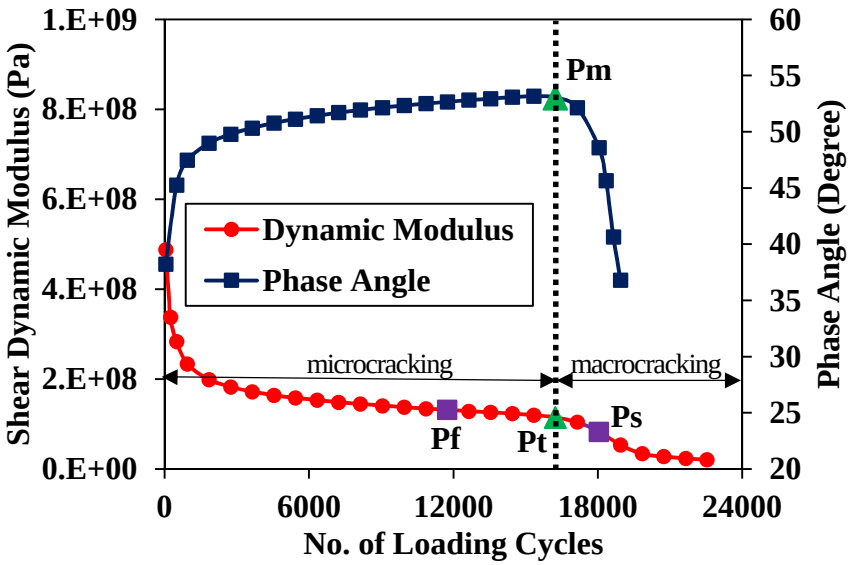

Figure 4.5. Dynamic shear modulus and phase angle vs. No. of loading cycles.

Regarding the time sweep test results, several studies (Kim and Little, 2005; Lee, 1996; Reese, 1997) investigated to identify a reasonable fatigue failure criterion. Lee (1996) indicated 50% loss in pseudo stiffness as the fatigue failure. Reese (1997) investigated fatigue failure based on changes in phase angle. Kim and Little (2005) performed time sweep tests on sand asphalt specimens containing different types of binders. They cross-plotted the number of loading cycles at the P_f, P_s, and P_t and number of loading cycles at the maximum phase angle (P_m), and calculated the total deviation error. They considered the total deviation error as the total absolute deviation from the line of equality. They found out that the number of loading cycles at the transition point showed

www.manaraa.com

the minimum deviation error from the maximum phase angle, and the number of loading cycles at P_t could be considered as an acceptable fatigue failure. Therefore, it could be inferred that the number of loading cycles at maximum phase angle was a fairly suitable fatigue failure criterion.

Phase angle of viscoelastic materials characterized viscous nature of the materials, and materials displayed more viscous behavior as the phase angle increased with more number of loading cycles because of microcrack generation. Consequently, the stiffness of the mixture decreased. When the phase angle reached its peak, microcracks coalescence into macrocracks, and it caused substantial loss of structural integrity within the specimen. This transition resulted in a significant drop of phase angle as shown in Figure 4.5.

In this study, the number of loading cycles at maximum phase angle (or the number of loading cycles at the transition point) was considered as the fatigue life of the mixture. Test results of the time sweep test were plotted on a log-log scale of the strain level versus the fatigue life for all mixtures as shown in Figure 4.6. The results noticeably illustrated that rejuvenators increased the fatigue life of mixtures, and the petroleum tech rejuvenated mixture showed greater fatigue resistance than the two other rejuvenated mixtures. Additionally, the mixture containing the petroleum tech rejuvenator and the WMA additive presented better fatigue resistance than the control mixture. These results strongly implied that rejuvenators and the WMA additive made mixtures softer and capable of accumulating more fatigue damage before failure because of the slow rate of stiffness reduction.

Furthermore, the results distinctly displayed that the control mixture had less fatigue resistance than the other mixtures especially at lower strain levels, and green and

www.manaraa.com

agriculture tech rejuvenated mixtures showed shorter fatigue lives than the petroleum tech rejuvenated mixture, especially at higher strain levels. Moreover, it could be seen that the control mixture, the petroleum tech rejuvenated mixture, and the mixture containing the WMA additive followed a similar trend of fatigue resistance at different strain levels.

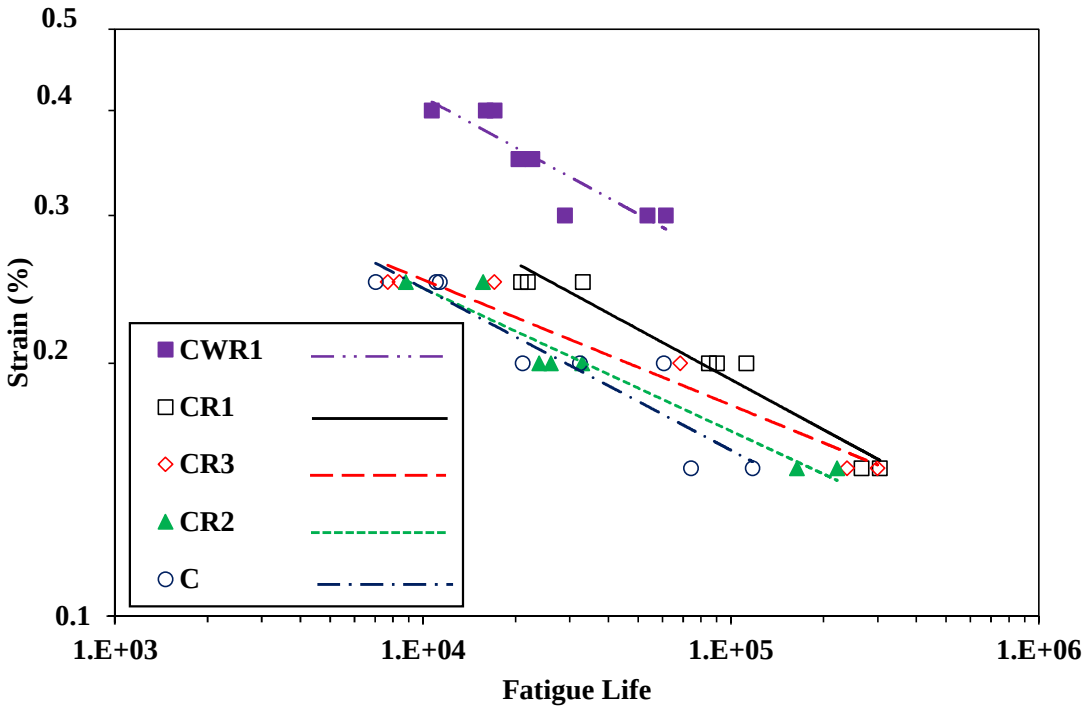

Figure 4.6. The strain level versus the fatigue life of each FAM mixture at 25˚C.

The amount of dissipated strain energy in each cycle and the total amount of dissipated strain energy (cumulative dissipated strain energy) during the time sweep test could be captured by taking inside area of the stress-strain hysteresis loop. Typical hysteresis stress-strain behavior is illustrated in Figure 4.7 with the results from CR2 mixture at a strain level of 0.15%. As it can be seen, the stress-strain loops shifted downward with the reduction of dissipated energy with increased loading cycles. The slope

www.manaraa.com

of the hysteresis loop showed the stiffness of the specimen at the corresponding number of loading cycles. It indicated that specimen showed lower stiffness as the number of loading cycles increased, and the specimen had nearly zero stiffness when it was close to the failure point. Additionally, the amount of cumulative dissipated strain energy (CDSE) at different strain levels for all FAM mixtures are presented in Figure 4.8. It can be implied that FAM mixtures with longer fatigue life could dissipate more energy to failure.

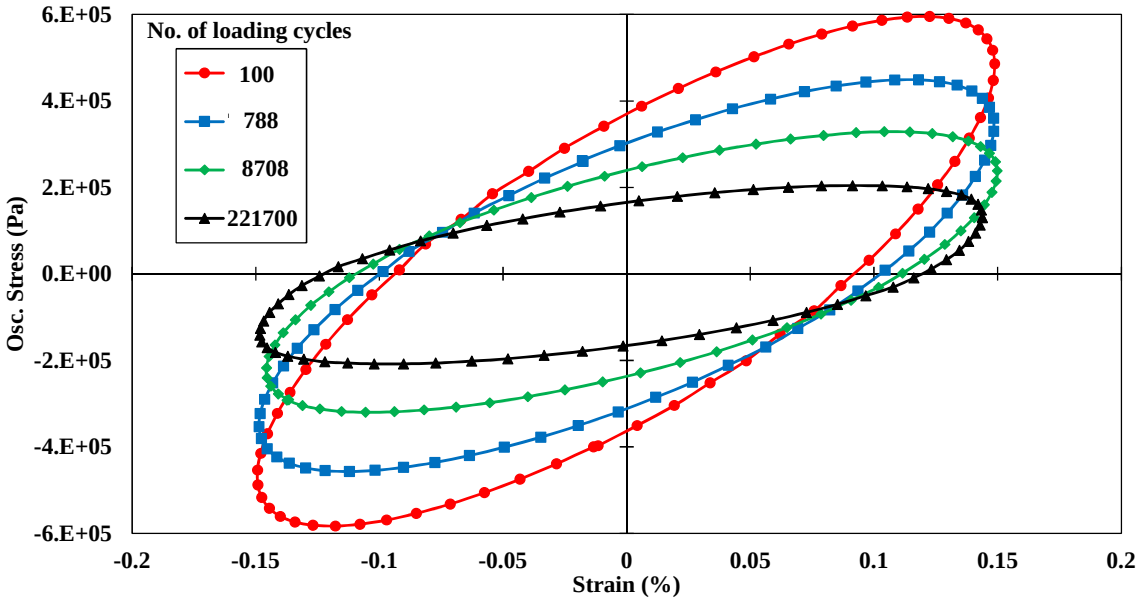

Figure 4.7. Stress-strain hysteresis loops with damage.

www.manaraa.com

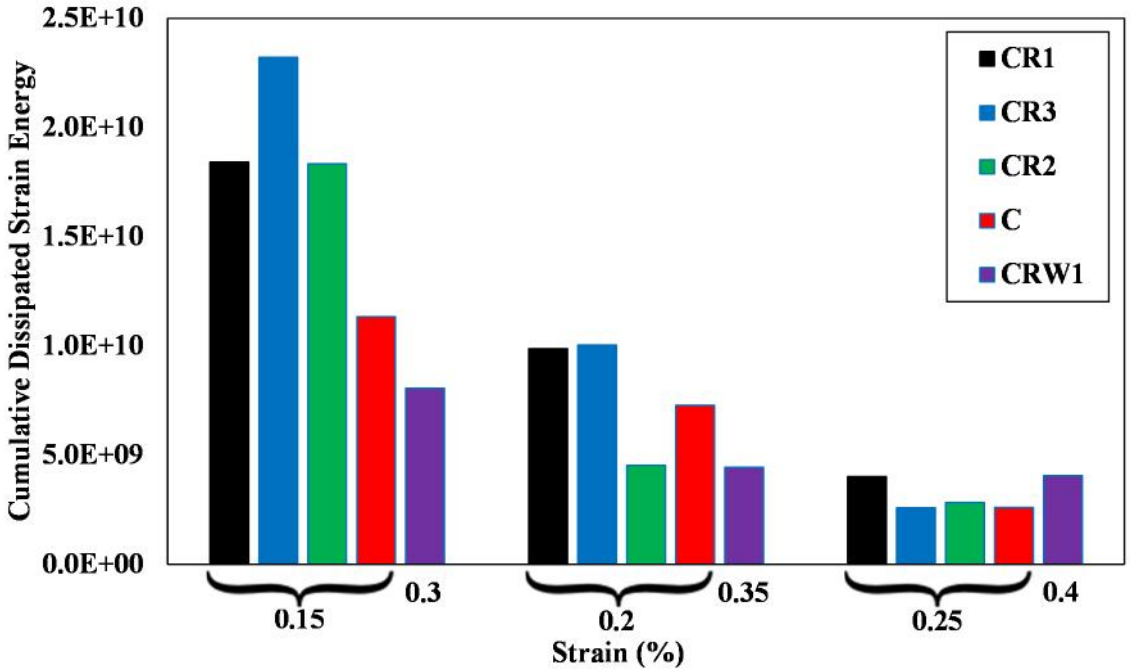

Figure 4.8. Cumulative dissipated strain energy for all mixtures. The strain levels to do time sweep tests on CRW1 mixture were different from other mixtures.

4.2.4. Static Creep-Recovery Test

Static creep-recovery tests were conducted to investigate stress-dependent permanent deformation characteristics of FAM mixtures. Thus, tests were performed at 40˚C. Creep loading time and recovery time were considered at 30 and 300 seconds, respectively. Tests were carried out in a wide range of creep stresses (i.e., 5, 15, 25, 50, and 75 kPa), and a static creep compliance, which was defined as the ratio of time-dependent strain to the applied static stress, was employed over the loading time to recognize the linear viscoelastic stress level in terms of homogeneity concept, which was described in section 0. Typical test results are presented in Figure 4.9 and Figure 4.10. Figure 4.9 illustrates that the linear viscoelastic region held until 15 kPa stress level, and after the linear viscoelastic stress level, creep compliance increased by increasing the applied stress level. Also,

www.manaraa.com

Figure 4.10 depicts that the higher stress levels than the linear viscoelastic stress level caused larger creep strain and showed less recovery at the testing temperature. It should be noted that the linear viscoelastic region for all mixtures held until 15 kPa stress level.

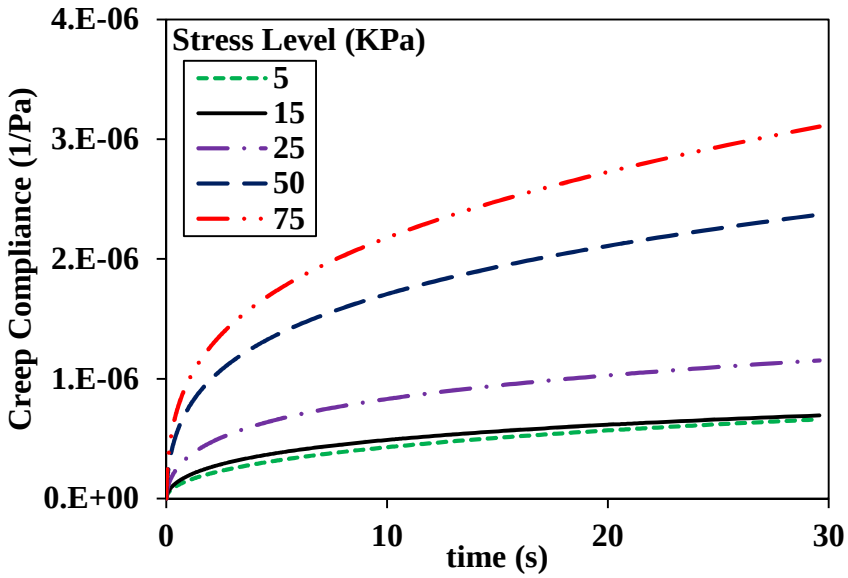

Figure 4.9. Creep test results to determine the linear viscoelastic stress level of the FAM mixture CR2.

www.manaraa.com

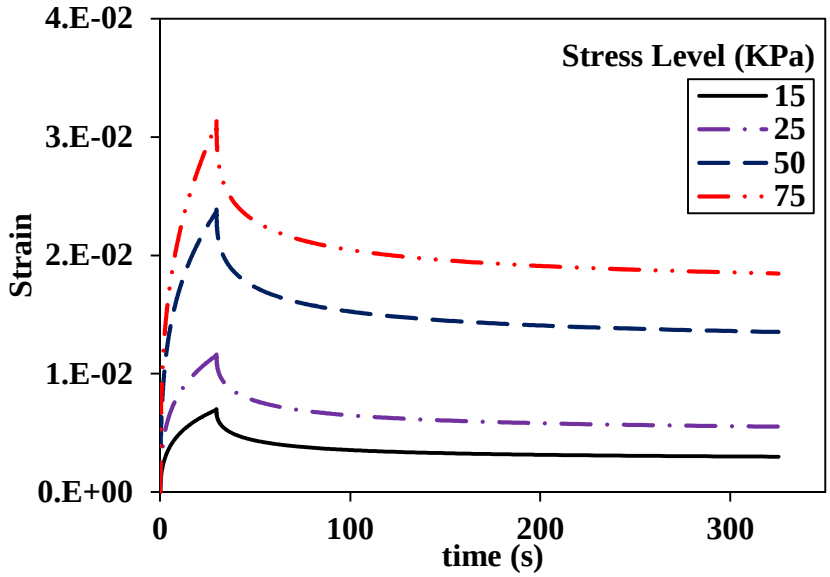

Figure 4.10. Creep-recovery test results of the FAM mixture CR2.

The creep and creep-recovery test results of all FAM mixtures at 25 kPa are compared in Figure 4.11 and Figure 4.12, respectively. The results indicated that the rejuvenated mixtures showed softer behavior than the control mixture as they could develop more strain, and the petroleum tech rejuvenator had more softening effect than the green tech and agriculture tech rejuvenators. Also, the mixture containing the WMA additive showed the softest behavior and the least recovery at the testing temperature. Test results were in good agreements with other test results (i.e., strain sweep and frequency sweep tests) presented earlier.

www.manaraa.com

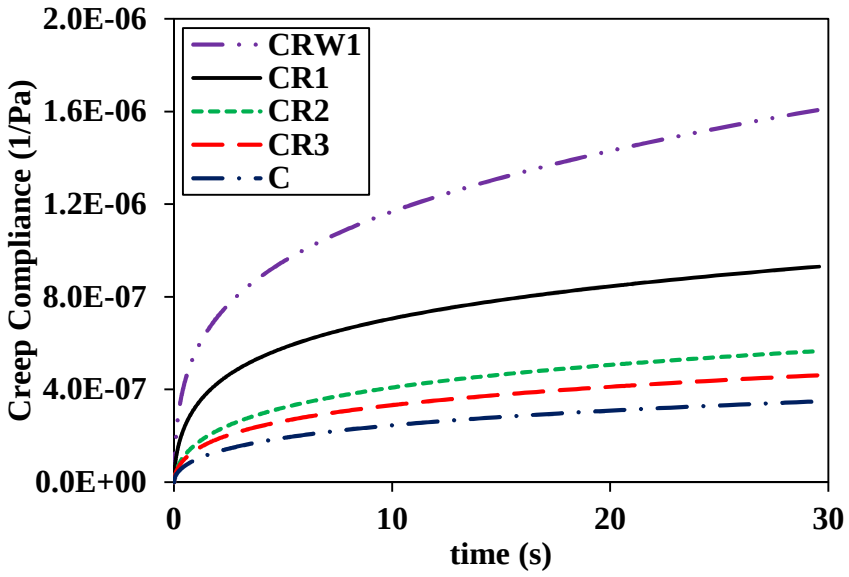

Figure 4.11. Creep test results of all mixtures at 25 kPa stress level.

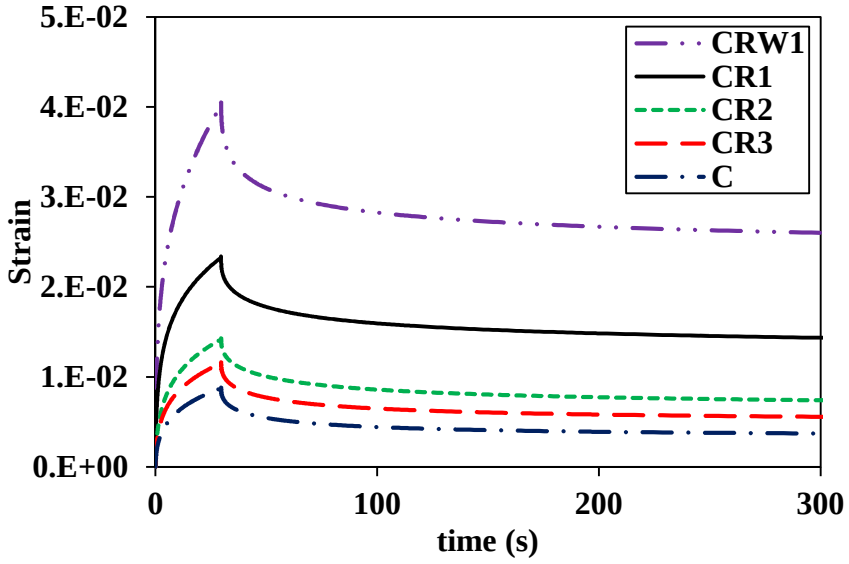

Figure 4.12. Creep test results of all mixtures at 25 kPa stress level.

www.manaraa.com

5. CHAPTER FIVE

ANALYSIS OF TEST RESULTS

5.1.Viscoelastic Characterization of Frequency Sweep Test Results

Static relaxation behavior of materials can be determined by results obtained from the torsional shear frequency sweep tests. Viscoelastic materials (FAM in this study) usually respond with mechanical characteristics under cyclic loading conditions such as phase angle between stress and strain due to material viscoelasticity, storage modulus because of the elastic characteristics, and loss modulus related to the viscous behavior. The combined form of these moduli (i.e., loss modulus and storage modulus) can be used to produce the phase angle, the dynamic modulus, and the complex modulus as indicated in Eq. 5.1 to Eq. 5.3.

$$¤(\mu) = \tan^{-1}\left[\frac{G''(\mu)}{G'(\mu)}\right] \qquad \textbf{Eq. 5.1}$$

$$\left|G^*(\mu)\right| = \frac{²_{max}}{¥_{max}} = \sqrt{\left[G'(\mu)\right]^2 + \left[G''(\mu)\right]^2} \qquad \textbf{Eq. 5.2}$$

$$G^*(\mu) = G'(\mu) + iG''(\mu) \qquad \textbf{Eq. 5.3}$$

where $¤(\mu)$ = phase angle,

$G'(\mu)$ = storage shear modulus,

$G''(\mu)$ = loss shear modulus,

$\left|G^*(\mu)\right|$ = dynamic shear modulus,

www.manaraa.com

$G^*(\mu)$ = complex shear modulus,

τ_{max} = maximum shear stress at each cycle,

γ_{max} = applied cyclic shear strain amplitude, and

$i = \sqrt{-1}$.

The dynamic shear modulus is described as the ratio of maximum shear stress to the maximum shear strain at each cycle as presented in Eq. 5.2; or it can be defined as an absolute value of the complex shear modulus, which is presented in Eq. 5.3. These equations can be used in both linear and non-linear viscoelastic behavior. Nonetheless, in order to determine the linear viscoelastic dynamic modulus, the maximum stress and the maximum strain or the storage modulus and the loss modulus need to be obtained within the linear viscoelastic region.

5.1.1. Master Curve Generation

Master curves are generated by considering time-temperature superposition principle and shifting frequency sweep test results to a certain temperature, which is called the reference temperature until the results superimposed to a single smooth curve. By using time-temperature superposition principle, a wide range of frequency was obtained and dynamic moduli of a mixture can be determined at extreme frequencies which are difficult to reach by performing traditional laboratory tests.

In this study, the reference temperature was set as 20˚C, and test results at 10˚C, 30˚C, and 40˚C were horizontally shifted towards the results at 20˚C until a single smooth curve was obtained. A master curve of test results performed on the FAM CR2 at reference temperature of 20˚C is exemplified in Figure 5.1. As it can be seen in the figure, the slope

www.manaraa.com

of a log-log scale plot of a linear viscoelastic dynamic modulus versus frequency is called *m*-value. The *m*-value is a well-known indicator related to fundamental viscoelastic material characteristics as reported by many studies including Kim and Little (2005).

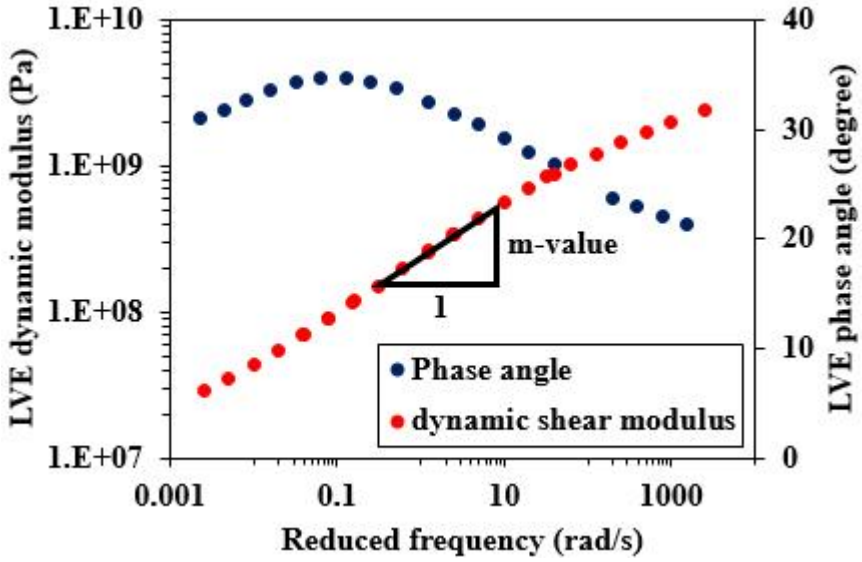

Figure 5.1. Linear viscoelastic dynamic modulus, phase angle, and the *m*-value of the FAM mixture CR2 at 20˚C.

The master curve of the phase angle is also illustrated in Figure 5.1. The phase angle is defined as the ratio of the loss modulus to the storage modulus as described in Eq. 5.1. Phase angles presented in Figure 5.1 infer that the difference between the loss modulus and the storage modulus decreased at intermediate loading frequencies and increased at low and high loading frequencies.

Master curves of all five different FAM mixtures at the reference temperature of 20˚C are illustrated in Figure 5.2. The results evidently showed that the rejuvenators and the WMA additive made the mixtures softer. The petroleum tech rejuvenator had the most

www.manaraa.com

softening effect among the three different rejuvenators, and the green tech and the agriculture tech rejuvenators nearly had same softening effect. Also, the control mixture showed the stiffest behavior, and the mixture containing the WMA additive and the petroleum tech rejuvenator showed the softest behavior among all five mixtures.

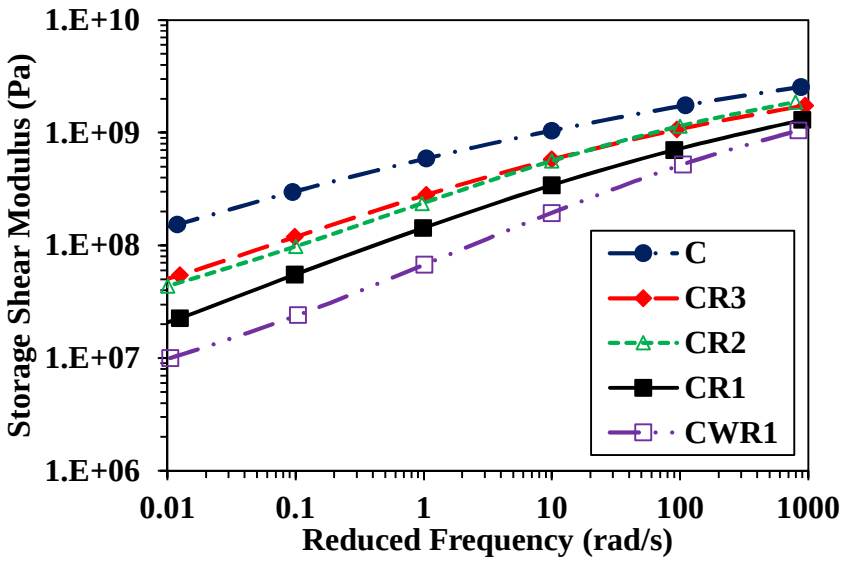

Figure 5.2. Storage modulus master curves of the five fine aggregate matrix at 20˚C.

Table 5.1 presents *m*-values of all FAM mixtures. The values in the table indicate that the rejuvenated mixtures relaxed stresses faster than the control mixture. Rejuvenated mixtures showed generally higher *m*-value than the control mixture.

www.manaraa.com

Table 5.1. Linear viscoelastic property (*m*-value) identified at the reference temperature, 20˚C.

Mixture	*m*-value
C	0.251
CR3	0.320
CR2	0.372
CR1	0.379
CRW1	0.463

5.1.2. Prony Series Curve Fitting

A curve fitting function can be used to fit the master curve generated from frequency sweep test results to characterize the linear viscoelastic relaxation modulus. The generalized Maxwell model where its mathematical expression is usually called a Prony series was used to find the curve fitting function, because it provides better efficiency in mathematical application and fits data more accurately than other models. Christensen (2012) presented Prony series presentations for the loss modulus and the storage modulus as a function of angular frequency as shown in Eq. 5.4 and Eq. 5.5.

$$G'(\omega) = G_{\infty} + \sum_{i=1}^{n} \frac{G_i \omega^2 \rho_i^2}{\omega^2 \rho_i^2 + 1} \qquad \textbf{Eq. 5.4}$$

$$G''(\omega) = \sum_{i=1}^{n} \frac{G_i \omega \rho_i}{\omega^2 \rho_i^2 + 1} \qquad \textbf{Eq. 5.5}$$

where G_{∞} = long term equilibrium shear modulus,

G_i = spring constants in the generalized Maxwell model,

ρ_i = relaxation times in the generalized Maxwell model,

www.manaraa.com

μ = frequency in radian,

n = number of dashpots in the generalized Maxwell model.

The spring constants could be determined by using a collocation method which is a matching process between the experimental data and the analytical representation at some different points. After the collocation process, resulting Prony series parameters are listed in Table 5.2.

Table 5.2. Prony series constants for all mixtures.

i	ρ_i (sec)	G_i (Pa)				
		C	CR3	CR2	CR1	CRW1
1	1000	4.35E+07	2.24E+07	1.98E+07	8.38E+06	3.52E+06
2	100	1.04E+08	3.64E+07	2.80E+07	1.69E+07	6.56E+06
3	10	2.11E+08	1.02E+08	8.00E+07	5.22E+07	2.11E+07
4	1	3.57E+08	2.15E+08	2.05E+08	1.27E+08	6.67E+07
5	0.1	5.63E+08	4.02E+08	4.46E+08	2.76E+08	1.94E+08
6	0.01	7.77E+08	5.90E+08	6.94E+08	4.73E+08	4.37E+08
7	0.001	1.04E+09	8.21E+08	1.05E+09	7.91E+08	7.83E+08
G_∞ (Pa)		5.00E+07	1.00E+07	1.00E+07	4.00E+06	3.00E+06

5.1.3. Static Relaxation Behavior

The static relaxation modulus as a function of loading time can then be obtained by using the same Prony series model parameters resulting from the Eq. 5.4 and Eq. 5.5, as the following equation.

$$G(t) = G_\infty + \sum_{i=1}^{n} G_i e^{-\frac{t}{\rho_i}} \qquad \textbf{Eq. 5.6}$$

www.manaraa.com

The static relaxation moduli of all mixtures are illustrated in Figure 5.3. As shown, rejuvenating additives typically softened the control mixture, and the rejuvenated mixture containing the WMA additive presented the softest behavior between all mixtures. Also, the petroleum tech rejuvenator made the mixture softer than the other two rejuvenators, and the green tech and the agriculture tech rejuvenators showed the similar effect on the mixtures.

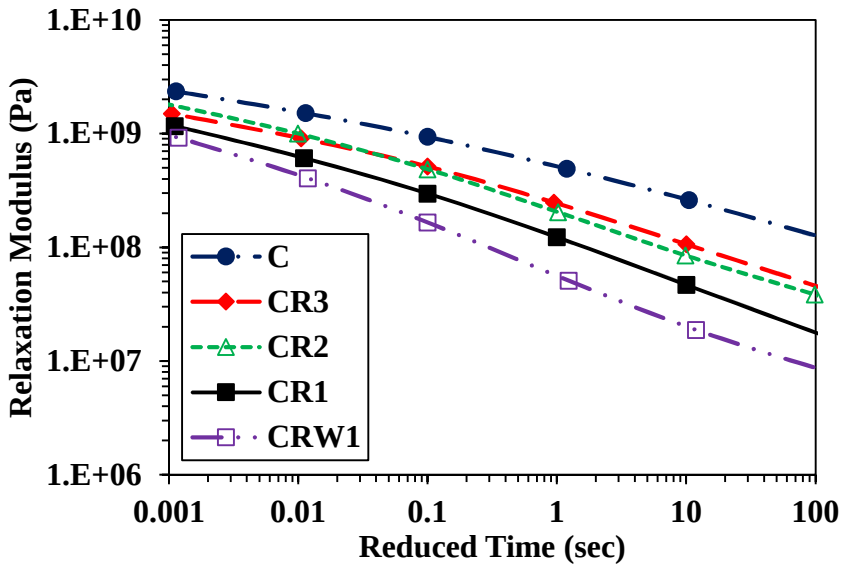

Figure 5.3. Relaxation modulus as a function of time for all mixtures.

5.2. Analysis of Time Sweep Test Results

Time sweep test results are described by two different approaches to examine fatigue damage resistance of each FAM mixture. The first approach is based on a simple phenomenological regression model, and the second approach is presented in the form of a mechanical fatigue life prediction model. These two approaches are explained in the following subsections.

www.manaraa.com

5.2.1. Phenomenological Regression Model

A phenomenological model is determined by a simple regression curve fitting. The time sweep test results are plotted on a log-log scale of the strain level versus the fatigue life. A same form of a regression model with different coefficients is obtained from the results as indicated in Eq. 5.7, and model coefficients are presented in Table 5.3. The table shows that as ~$_1$ increases and $_1$ decreases, the fatigue life of FAM increases. Using the model, fatigue life of all FAM mixtures are determined and cross plotted in Figure 5.4.

$N_f = \sim_1 (¥)^{-\ 1}$ **Eq. 5.7**

where N_f = fatigue life,

¥ = applied shear strain amplitude, and

~$_1$, $_1$ = regression constants.

Table 5.3. Phenomenological fatigue life model coefficients.

Mixture	α_1	β_1
C	2.00E-07	4.69
CR2	7.00E-06	4.29
CR3	2.50E-05	3.53
CR1	2.40E-04	3.31
CRW1	4.00E-04	2.15

www.manaraa.com

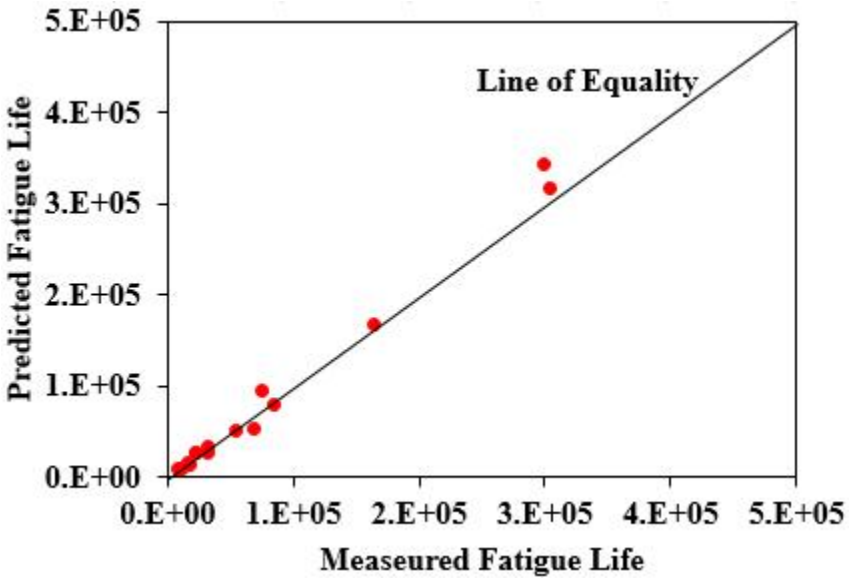

Figure 5.4. Predicted fatigue life versus measured fatigue life, using the phenomenological model.

5.2.2. Mechanistic Fatigue Life Prediction Model

A fatigue life model was proposed by Lee et al. (2000) through the continuum damage mechanics and work potential theory for asphalt concrete specimens under uniaxial cyclic loading. Kim and Little (2005) adopted the model on data from torsional shear cyclic loading tests without rest periods in two different ways. One, by using dissipated pseudo strain energy and pseudo stiffness, and the other by using dissipated strain energy. In this study, the mechanistic fatigue life prediction model based on the dissipated strain energy was employed to characterize the fatigue behavior of the different FAM mixtures. The model is presented in the same form of the phenomenological regression model with model parameters which are represented by several material properties and damage characteristics as shown in Eq. 5.8.

www.manaraa.com

$N_f = \sim_2 (¥)^{\,2}$ **Eq. 5.8**

where $\sim_2 = \dfrac{f(D_f)^k}{k\left(® \dfrac{I_D}{\left|G^*(\mu)\right|} C_1 C_2\right)^{\sim} \left|G^*(\mu)\right|^{\sim}}$

$_2 = 2\sim$

$f =$ loading frequency, in this study 10 Hz,

$D_f =$ damage parameter when the sample approaches fatigue failure,

$k = 1 + (1 - C_2)\sim$,

$I_D =$ initial nonlinear dynamic modulus, which is used to eliminate sample to sample variability,

$\left|G^*(D)\right| =$ linear viscoelastic dynamic shear modulus,

$C_1, C_2 =$ regression constants, and

$\sim$ = a material constant.

The regression constants (i.e., C_1, C_2) could be determined using the curve of $G"$(D) versus D, which typically follows a power relation as presented in Eq. 5.9.

$G"(D) = C_0 - C_1 (D)^{C_2}$ **Eq. 5.9**

where $G"(D) =$ damage-induced loss modulus at each cycle,

$D =$ damage parameter, and

$C_{0,} C_1, C_2 =$ regression constants.

www.manaraa.com

At first, the material constant ($\sim$) is assumed and then varied until cross-plotting the measured G'' and D at several different strain levels results in closure. Based on Schapery (1975), $\sim$ is related to the material's relaxation or creep properties. If $\sim$ is a true material property, the load level dependency is eliminated. Also, damage parameter D is calculated using Eq. 5.10.

$$D \cong \sum_{i=1}^{N}\left[\text{®} I_D (\text{¥}_i)^2 (G''_{i-1} - G''_i) \right]^{\frac{\sim}{\sim+1}} (t_i - t_{i-1})^{\frac{1}{1+\sim}} \qquad \textbf{Eq. 5.10}$$

where N is the total number of loading cycles.

As mentioned, $\sim$ is determined by a calibration process to eliminate the load level dependency. Figure 5.5 and Figure 5.6 illustrate cross-plots of the damage-induced loss modulus with increasing damage parameter before and after strain level dependency is eliminated by changing the $\sim$ value. The figures depicted that an appropriate value of $\sim$ could effectively remove the load level dependency. Resulting model parameters can then be identified by using Eq. 5.8 to Eq. 5.10, and are presented in Table 5.4. Table 5.4 indicates that mixtures with greater fatigue resistance can accumulate more damage to fatigue failure, which results in larger value of damage parameter, D.

www.manaraa.com

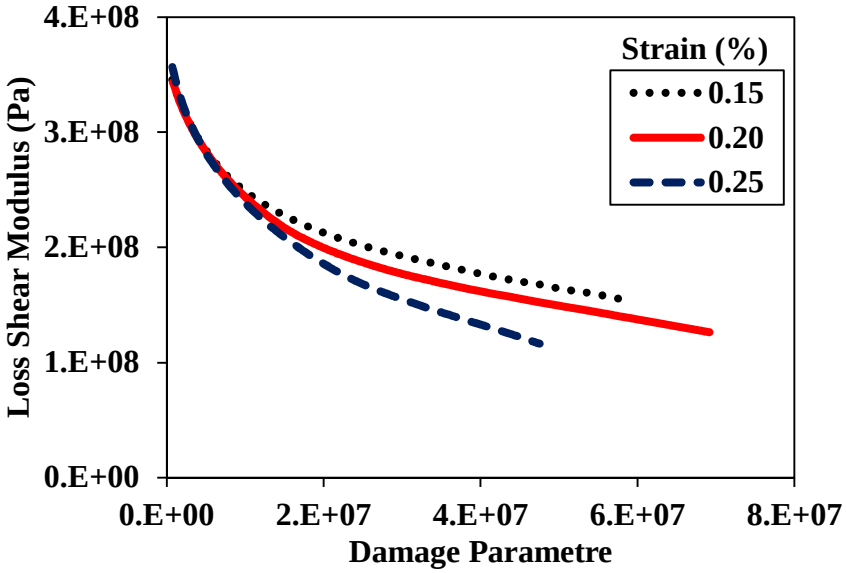

Figure 5.5. Damage-induced loss modulus at each cycle versus calculated damage parameter before elimination of strain level dependency.

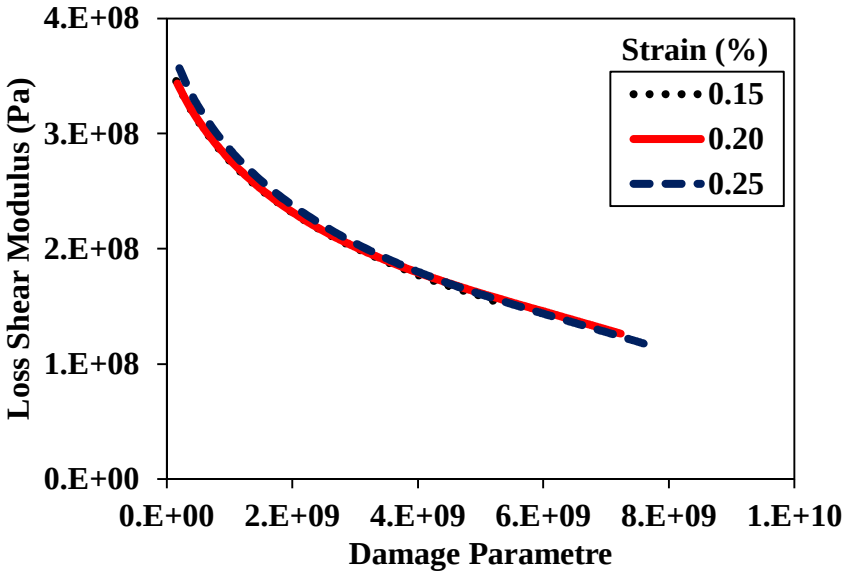

Figure 5.6. Damage-induced loss modulus at each cycle versus calculated damage parameter after elimination of strain level dependency.

www.manaraa.com

Table 5.4. Mechanistic fatigue life prediction model parameters.

Mixture	I_D (GPa)	$\left\|G^*\right\|$ (GPa)	~	k	D_f
C	0.678	1.193	2.4	3.055	906,314,391
CR2	0.423	0.866	2.1	2.688	1,120,482,489
CR3	0.437	0.824	1.7	2.421	1,875,504,413
CR1	0.229	0.527	1.6	2.005	1,922,874,677
CRW1	0.125	0.307	1.1	1.663	2,215,545,091

The estimated fatigue lives using the mechanistic model are cross-plotted to the measured fatigue lives as illustrated in Figure 5.7. Fairly good agreement was found between the estimated and predicted fatigue lives, which attests to the validity of the mechanistic fatigue model.

The mechanistic fatigue model is considered more advantageous and informative than the simple phenomenological regression model, since the mechanistic model is represented as functions of damage-induced parameters as well as fundamental material properties. Model parameters provide the potential to explain fatigue damage mechanisms more clearly and to investigate how fundamental material properties affect fatigue life. By evaluating model parameters, one can select better materials that are more resistant to fatigue damage.

www.manaraa.com

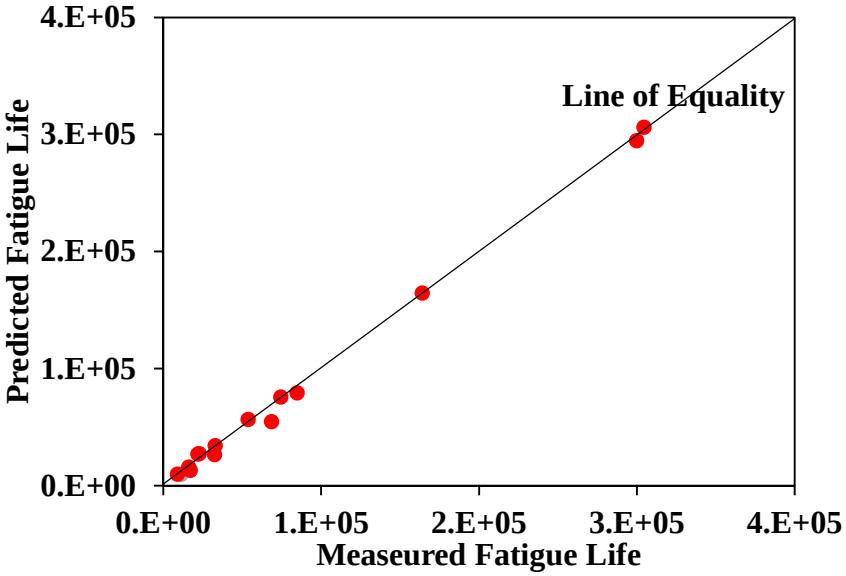

Figure 5.7. Predicted fatigue life versus measured fatigue life using the mechanistic prediction model.

5.2.3. Comparison of phenomenological and mechanistic fatigue life models

Phenomenological and mechanistic fatigue life prediction model parameters are provided in Table 5.5. It can be seen that both models had similar values of the model parameters. As the α value increased, the fatigue resistance increased, and as the β decreased, the mixtures showed longer fatigue life. As mentioned, in the phenomenological model, parameters were obtained from a simple curve fitting, while the mechanistic model parameters were identified by material properties and damage evolution characteristics. This can potentially provide insights into the effects of fundamental material properties on the overall mixture fatigue resistance so that users can select and/or design better materials related to fatigue damage.

www.manaraa.com

Table 5.5. Phenomenological and mechanistic fatigue life prediction model parameters.

Mixture	Phenomenological model		Mechanistic model	
	$\sim_1$	$_1$	$\sim_2$	$_2$
C	2.00E-07	4.69	2.70E-07	4.80
CR2	7.00E-06	4.29	6.67E-06	4.20
CR3	2.50E-05	3.53	3.33E-05	3.40
CR1	2.40E-04	3.31	1.41E-04	3.20
CRW1	4.00E-04	2.15	3.36E-04	2.20

5.3. Static Creep-Recovery Test Results Analysis

Figure 5.8 schematically illustrates a static creep-recovery test, and it shows three time dependent strain: $\pounds_C(t)$ as the total amount of strain, $\Delta\pounds_r(t)$ as the recoverable amount of strain, and $\pounds_r(t)$ as the irrecoverable amount of strain. These parameters could be used as inputs for viscoelastic and viscoplastic models (e.g., Schapery's viscoelastic model, Perzyna's viscoplastic model). Using the static creep-recovery test results, the amount of creep strain ($\pounds_C(t_1)$) and irrecoverable strain ($\pounds_r(t_2)$) were determined for all FAM mixtures at different stress levels as illustrated in Figure 5.9 and Figure 5.10.

www.manaraa.com

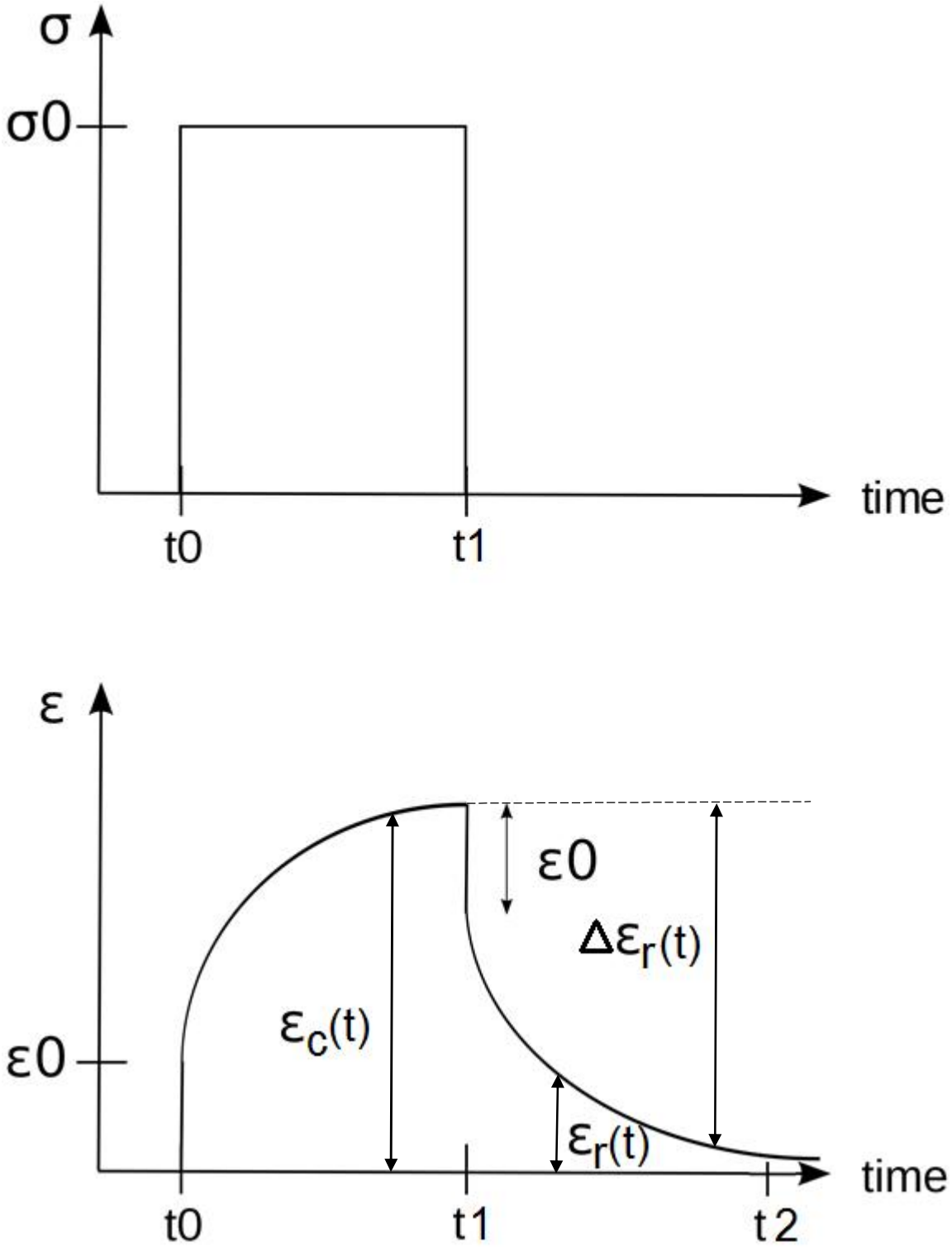

Figure 5.8. A single creep-recovery test.

www.manaraa.com

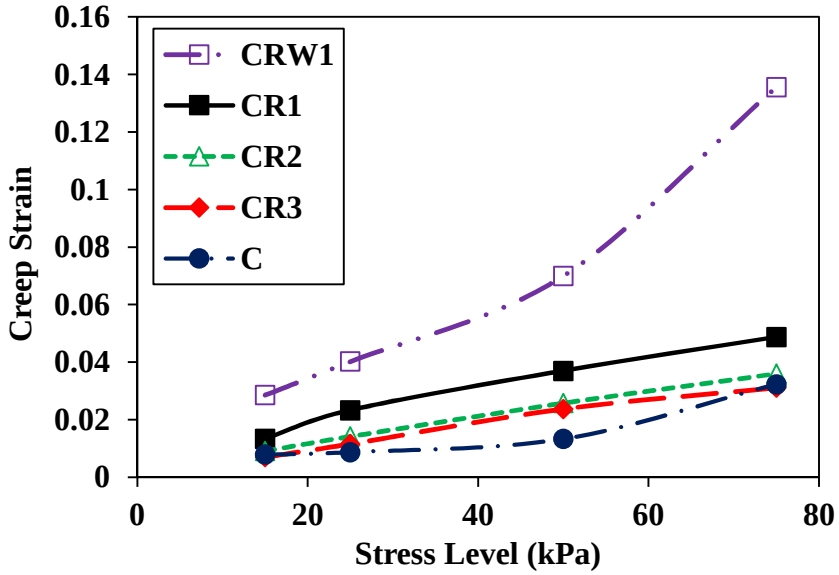

Figure 5.9. Creep strain for all FAM mixtures at different stress levels.

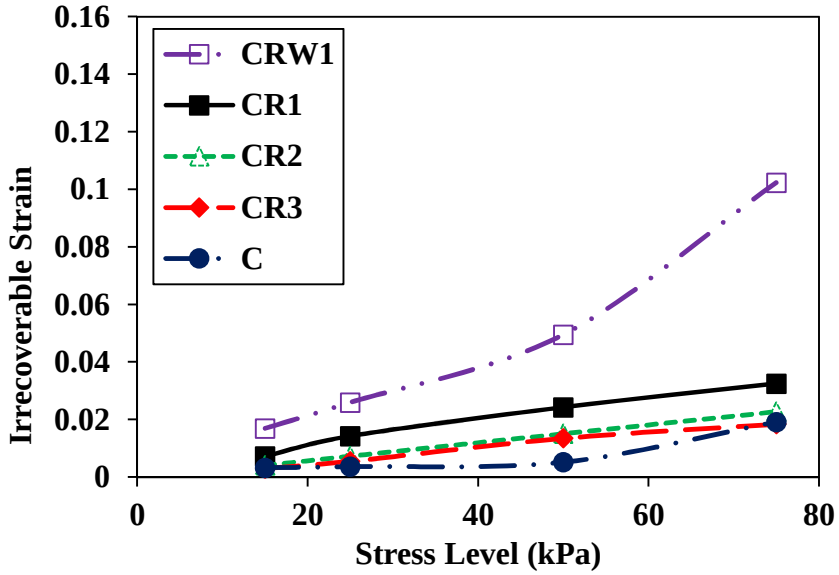

Figure 5.10. Irrecoverable strain for all FAM mixtures at different stress levels.

www.manaraa.com

The figures depicted that the amount of creep strain and irrecoverable strain increased as the applied stress increased. Also, FAM mixtures with softer behavior showed more amounts of creep strain and irrecoverable strain. It can be implied that increasing the softening behavior of FAM mixtures can result in more rutting potential due to increased amount of irrecoverable strain.

www.manaraa.com

6. CHAPTER SIX

LINKAGE BETWEEN FAM MIXTURES AND ASPHALT CONCRETE MIXTURES

This chapter explores a linkage between performance characteristics of the asphalt concrete mixture and its corresponding FAM phase by comparing experimental test results of asphalt concrete mixture and FAM phase. Test results were compared by considering three different aspects: stiffness, fatigue cracking, and permanent deformation.

Frequency sweep test results of asphalt concrete mixture and FAM mixture were compared to evaluate a linkage between stiffness of the two length scales. Also, test results of semicircular bending (SCB) test of asphalt concrete mixture were compared with time sweep test results of FAM mixture to explore fatigue cracking linkage. Finally, permanent deformation linkage was examined using flow number test results of asphalt concrete mixture and creep test results of FAM mixture.

It should be noted that the asphalt concrete mixture test results were obtained from another research study which was performed at the same time of this study in the Geomaterials Laboratory at the University of Nebraska-Lincoln.

6.1. Stiffness Linkage of AC mixture and FAM

Stiffness characteristic of asphalt concrete mixture and its corresponding FAM phase was evaluated by performing frequency sweep test on both length scales. Frequency sweep test on asphalt concrete specimen was performed at three test temperatures: 4˚C, 20˚C, and 40˚C. Using the test results, master curves of dynamic modulus, phase angle, storage

www.manaraa.com

modulus, and loss modulus were plotted at 20˚C as they are presented in Figure 6.1 (b), Figure 6.2 (b),Figure 6.3 (b), and Figure 6.4 (b). Also, frequency sweep test on FAM specimen was conducted as described in section 0, and test results were used to obtain master curves of dynamic shear modulus, phase angle, storage shear modulus, and loss shear modulus at 20˚C as illustrated in Figure 6.1 (a)Figure 6.2 (a)Figure 6.3 (a), and Figure 6.4 (a).

The asphalt concrete mixture test results showed that the petroleum tech rejuvenated mixture was softest, and the control mixture was the stiffest. Mixtures containing agriculture tech and green tech rejuvenators showed similar behavior. The test results of FAM mixture demonstrated that the control mixture and the petroleum tech rejuvenated mixture showed the stiffest and the softest behavior, respectively. The green tech and the agriculture tech rejuvenators showed similar softening effect on FAM. Therefore, asphalt concrete mixture and FAM mixture test results were in generally good agreement each other.

www.manaraa.com

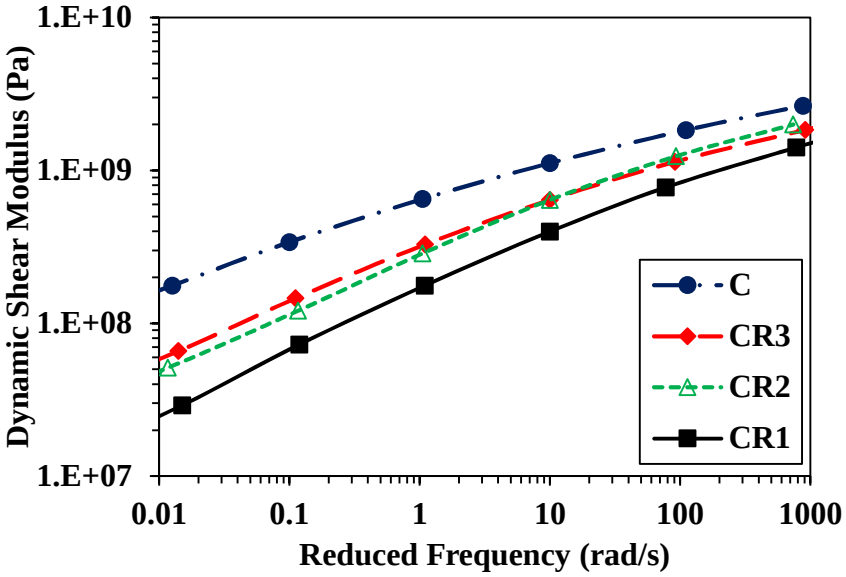

(a)

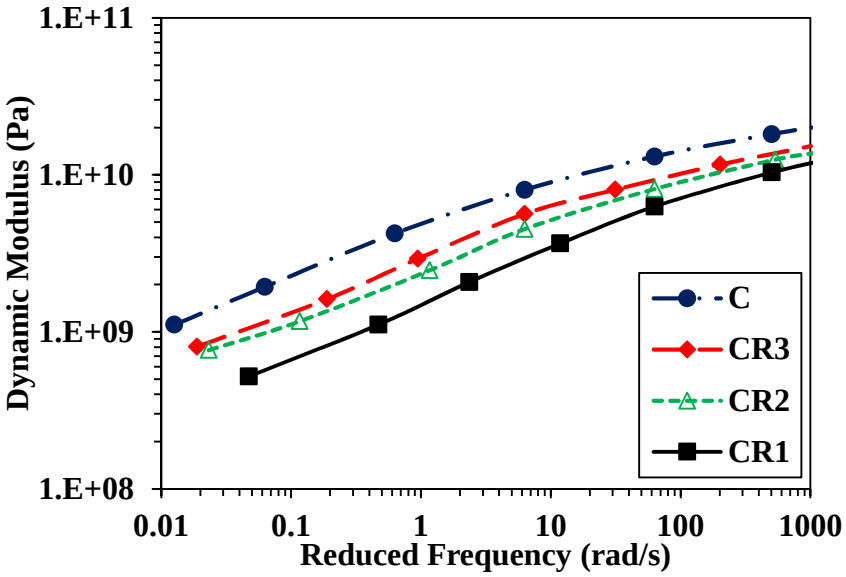

(b)

Figure 6.1. Dynamic modulus test results of (a) FAM mixtures (b) asphalt concrete mixtures.

www.manaraa.com

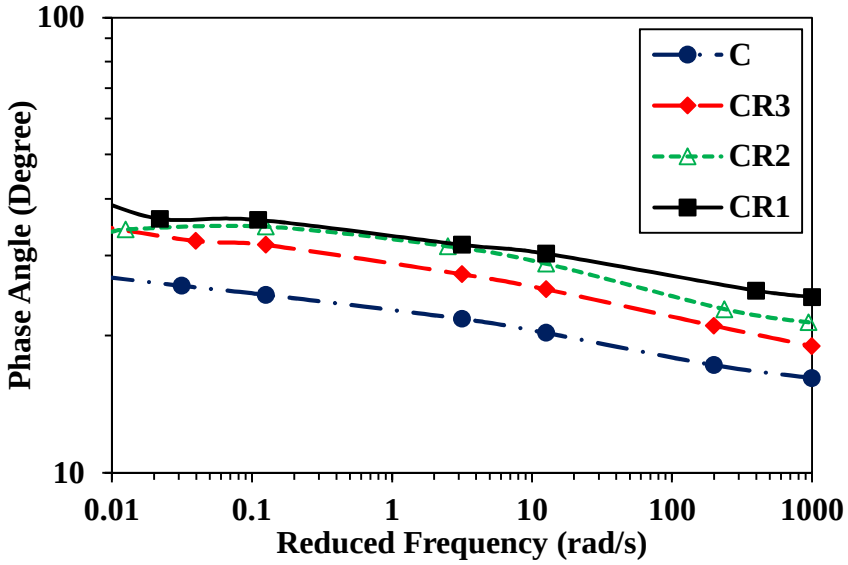

(a)

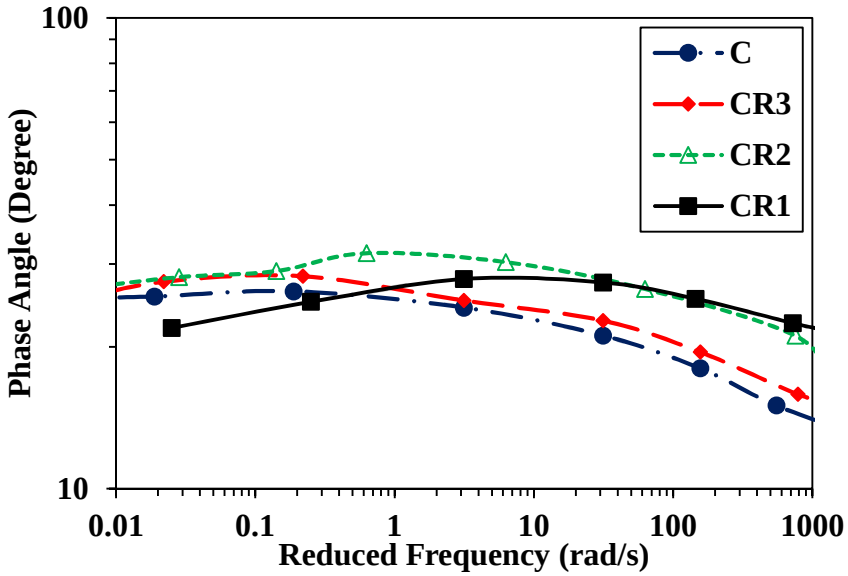

(b)

Figure 6.2. Phase angle test results of (a) FAM mixtures (b) asphalt concrete mixtures.

www.manaraa.com

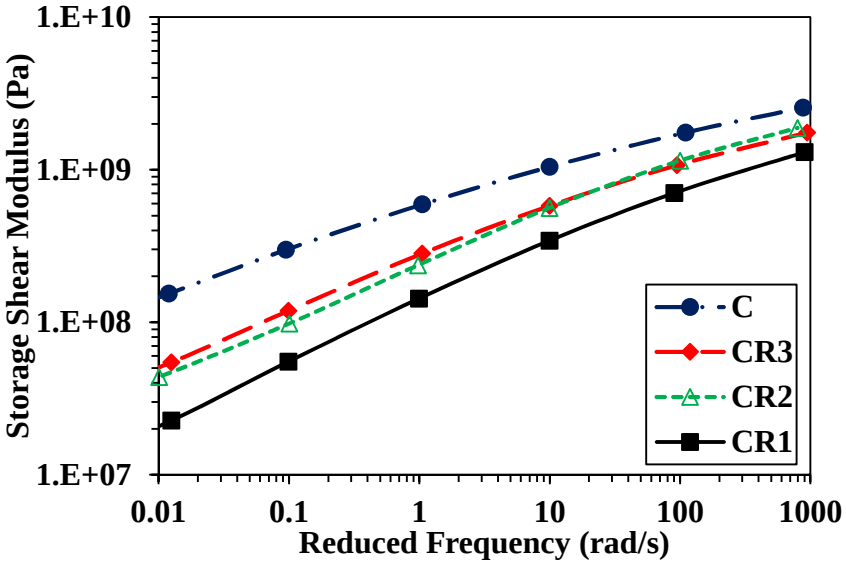

(a)

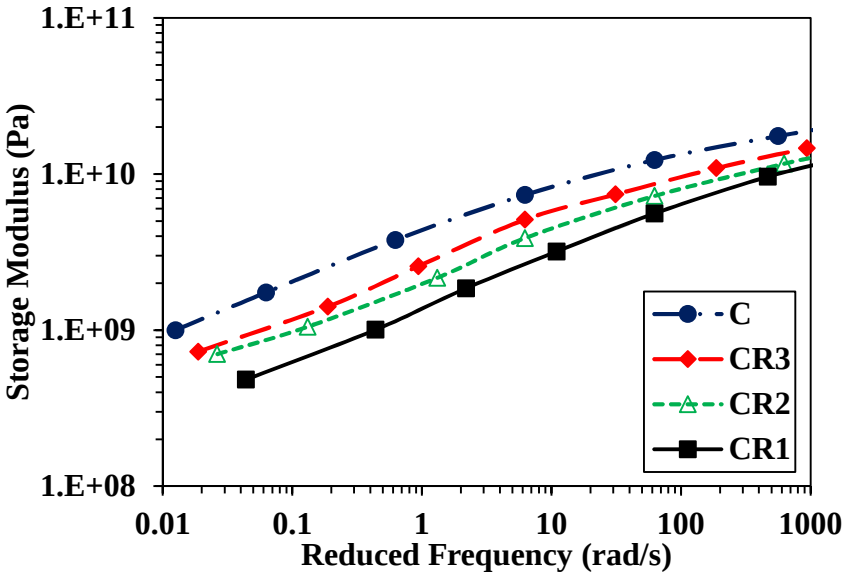

(b)

Figure 6.3. Storage modulus test results of (a) FAM mixtures (b) asphalt concrete mixtures.

www.manaraa.com

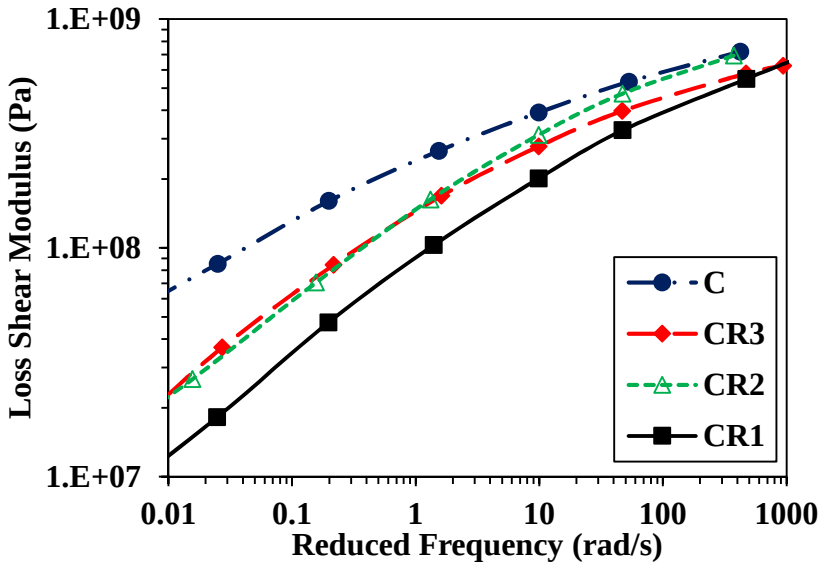

(a)

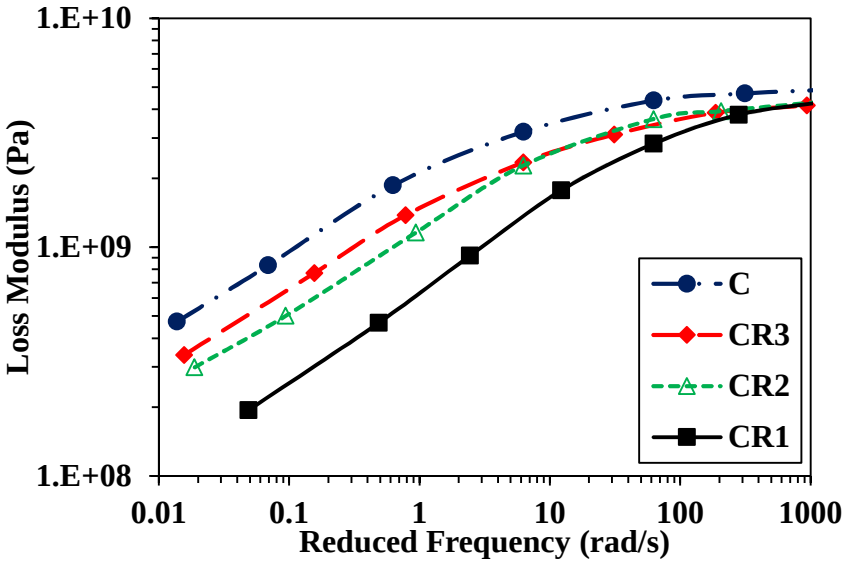

(b)

Figure 6.4. Loss modulus test results of (a) FAM mixtures (b) asphalt concrete mixtures.

www.manaraa.com

6.2. Fatigue Cracking Linkage of AC Mixture and FAM

Time sweep test results of FAM mixtures were compared with test results of semicircular bending test of asphalt concrete mixtures to explore a linkage in cracking behavior between the two length scales. Although both tests targeted mixture failure due to cracking, it should be noted that the time sweep test of FAM specimens was performed using a torsional shearing mechanism, while the semicircular bending test of asphalt concrete mixture specimens was conducted to induce opening mode cracking and failure.

In order to explore a linkage between the two, a cracking-related indicator of the semicircular bend fracture test was necessary so that it can be compared to the time sweep fatigue test results (such as fatigue life) of FAM mixtures. To this end, four indicators resulting from the semicircular bending fracture test were investigated. They include the peak load, the fracture energy which is defined as the area beneath the load-displacement curve, the pre-peak slope in the load-displacement curve, and the post-peak slope in the load-displacement curve.

Among the four potential indicators, the post-peak slope presented a good correlation with the FAM fatigue test results, as illustrated in Figure 6.5. This observation seems reasonable, because the post-peak slope in the semicircular bend fracture test represents the mixture's rate of damage which is particularly due to fracture.

The absolute values of the post-peak slopes are presented in Table 6.1. Test results of asphalt concrete mixture and FAM mixture showed that as the absolute value of post-peak slope increased, the fatigue life decreased.

www.manaraa.com

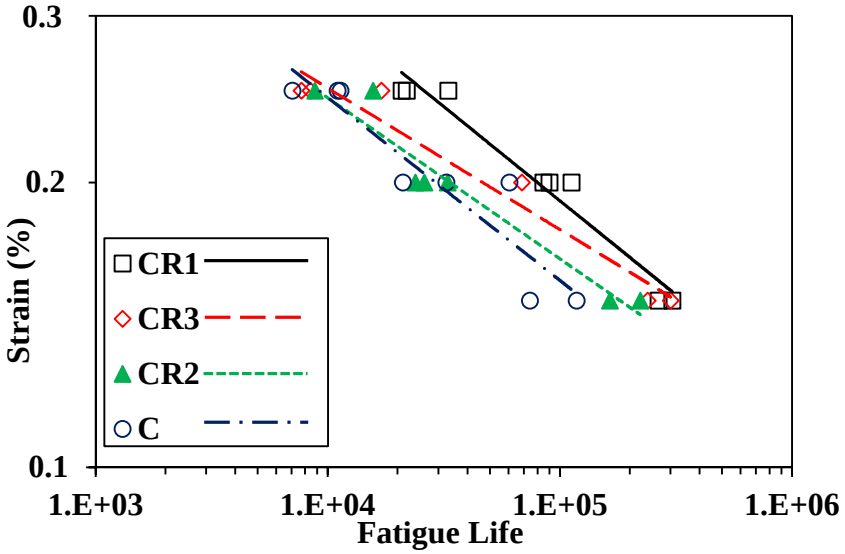

(a)

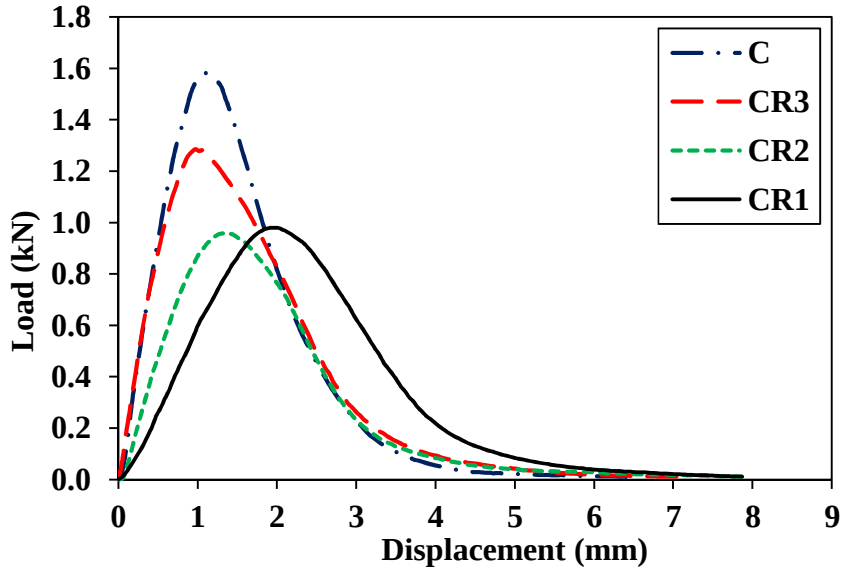

(b)

Figure 6.5. Results of (a) time sweep tests of FAM mixture (b) semicircular bending tests of asphalt concrete mixture.

www.manaraa.com

Table 6.1. The absolute value of the post peak slope of semi-circular bending test results of asphalt concrete mixtures, load versus displacement.

Mixture	Post peak slope
C	1.063
CR3	0.605
CR2	0.613
CR1	0.480

6.3. Permanent Deformation Linkage of AC Mixture and FAM

Permanent deformation linkage was evaluated by comparing results of flow number test of asphalt concrete mixtures and static creep test of FAM mixtures. Flow number tests were performed on the asphalt concrete cylinders at 40˚C with 138 kPa uniaxial pressure. Loading time and rest period were 0.1 and 0.9 seconds. Tests were continued until 10,000 cycles or 100,000 seconds. Test results are presented in Figure 6.6 (b). Flow number test results of asphalt concrete mixtures were compared with the static creep test results of FAM mixtures at stress level of 75 kPa. As shown in Figure 6.6, both tests yielded the same rank order of permanent deformation among the four mixtures. As expected, the control mixture experienced the lowest amount of permanent deformation, while other rejuvenated mixtures presented larger strains due to more compliant mixture characteristics. It can also be noted that the effects of rejuvenating agents (in particular CR2 and CR3) on permanent deformation of each mixture scale (i.e., asphalt concrete vs. FAM) were not same, as seen in the figures. This observation remains further investigation to explain why.

www.manaraa.com

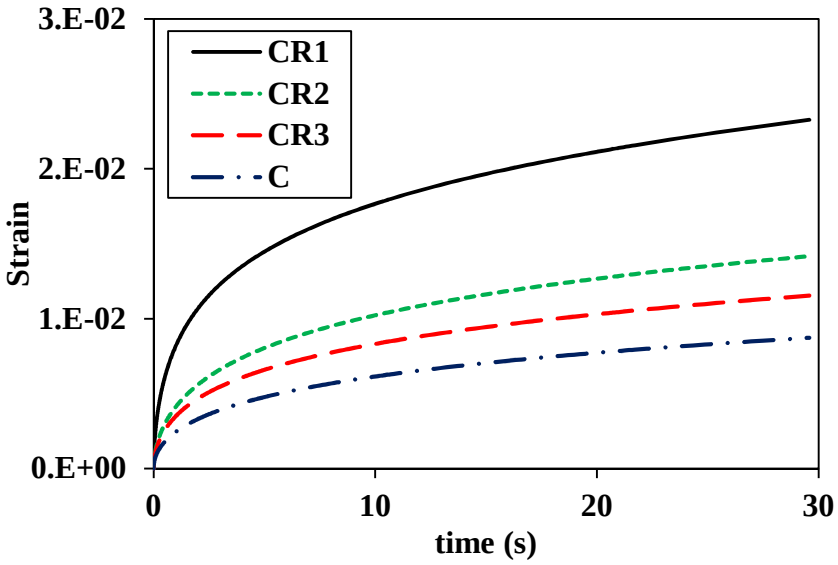

(a)

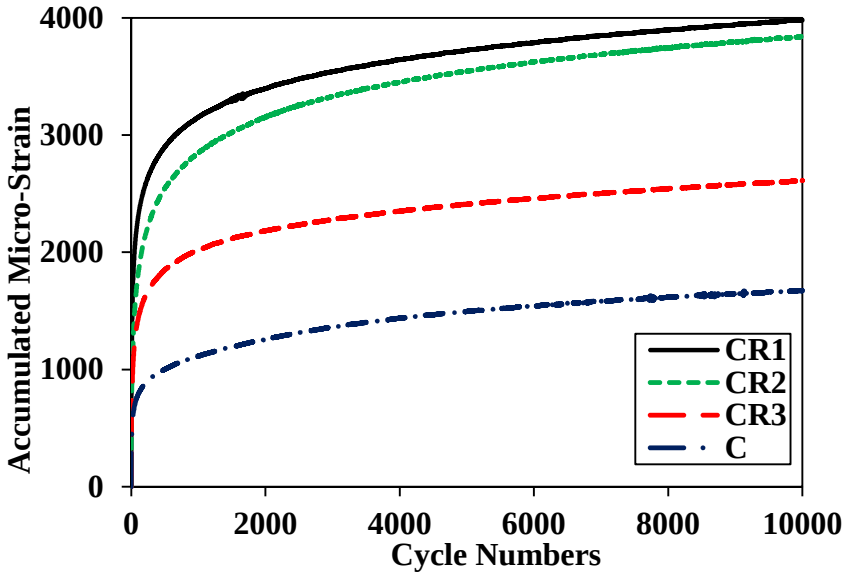

(b)

Figure 6.6. Results of (a) creep test of FAM mixture (b) flow number of asphalt concrete mixtures.

www.manaraa.com

7. CHAPTER SEVEN

CONCLUSIONS AND RECOMMENDATIONS

7.1. Summary and Conclusions

This study presents performance characteristics of different mixtures containing 65% RAP, three different types of rejuvenators (i.e., petroleum tech, green tech, and agricultural tech), and one WMA additive. This was done by performing various torsional shear tests of different FAM mixtures using a dynamic mechanical analyzer, and FAM test results were then compared with the corresponding test results of the entire (asphalt concrete) mixtures. Based on the test-analysis results, the following conclusions can be drawn.

- Dynamic mechanical analysis can be efficiently used to characterize viscoelastic material properties, the fatigue behavior, and the permanent deformation characteristics of FAM mixtures in a torsional shear mode.
- FAM allows much smaller geometry and more homogeneous nature than the entire asphalt concrete mixture. These advantages result in FAM testing being efficient and simple. In addition, FAM testing reduces costs and time compared to testing of the entire asphalt concrete mixture.
- Evaluation of linear viscoelastic material properties (i.e., static relaxation behavior) of FAM distinctly specifies substantial softening effects due to rejuvenators and the WMA additive. Test results showed that the petroleum tech rejuvenator provides greater softening effect than other two rejuvenators evaluated in this study, and the petroleum

www.manaraa.com

tech rejuvenated mixture with the WMA additive presented the softest behavior among all mixtures with decreased mixing-compaction temperatures.

- Rejuvenated mixtures could increase fatigue life of the control mixture under the strain-controlled fatigue testing mode. Fatigue test results were then used for the mechanistic fatigue life prediction model, which confirms that the rejuvenators can improve the fatigue cracking resistance of the high-RAP mixture by allowing the mixture to dissipate more energy until fatigue failure.
- The multiple stress creep-recovery tests of FAM mixtures presented the stress-dependent permanent deformation characteristics of mixtures and the effects of rejuvenators and WMA additive on deformation characteristics with different levels due to different types and dosages of the additives.
- Comparing test results from asphalt concrete mixtures and its corresponding FAM mixtures demonstrates a linkage between the two length scales in viscoelastic stiffness characteristics, fatigue cracking potential, and permanent deformation characteristics. Although further investigations are necessary to reach any definite conclusions, observations found in this study imply that the asphalt concrete mixture characteristics can hypothetically be predicted (or estimated) from FAM testing which would significantly save experimental efforts required to perform asphalt concrete testing.

7.2. Recommended Future Work

The following future work can be recommended.

- In this study, the amount of binder to fabricate FAM specimens was determined based on a reasonable assumption, because any certain procedures for FAM design have not

www.manaraa.com

been proposed yet. It would be recommended to develop such a rigorous mixture design and fabrication procedure based on a more scientific linkage between FAM and its corresponding asphalt concrete mixture so that the FAM test results can better represent the entire asphalt concrete behavior.

- In this study, FAM specimens were compacted manually with a static pressure applied into a cylindrical mold. In order to reduce variation due to the manual compaction, an automatic compaction process with a pneumatic pressure has been designed and developed. The compaction device is not ready for use yet, but its development will be completed for actual fabrication.
- The linkage between asphalt concrete mixture and its corresponding FAM phase needs further investigation. This requires extended test-analysis with different mixtures, testing conditions, and relevant constitutive theories such as viscoelasticity, viscoplasticity, continuum damage mechanics and/or fracture mechanics.

www.manaraa.com

REFERENCES

Al-Qadi, I.L., Aurangzeb, Q., Carpenter, S.H., Pine, W.J. and Trepanier, J., 2012. Impact of high RAP contents on structural and performance properties of asphalt mixtures. FHWA-ICT-12-002.

Austerman, A.J., Mogawer, W.S. and Bonaquist, R., 2009. Investigation of the influence of warm mix asphalt additive dose on the workability, cracking susceptibility, and moisture susceptibility of asphalt mixtures containing reclaimed asphalt pavement, proceedings of the fifty-fourth annual conference of the canadian technical asphalt association (ctaa); moncton, nb november, 2009.

Branco, C. and Franco, V.T., 2009. A unified method for the analysis of nonlinear viscoelasticity and fatigue cracking of asphalt mixtures using the dynamic mechanical analyzer.

Goh, S.W. and You, Z., 2011. Mechanical properties of porous asphalt pavement materials with warm mix asphalt and RAP. Journal of Transportation Engineering.

Im, S., 2012. Characterization of viscoelastic and fracture properties of asphaltic materials in multiple length scales.

Im, S., You, T., Ban, H. and Kim, Y.-R., 2015. Multiscale testing-analysis of asphaltic materials considering viscoelastic and viscoplastic deformation. International Journal of Pavement Engineering(ahead-of-print): 1-15.

Im, S. and Zhou, F., 2014. Field Performance of RAS Test Sections and Laboratory Investigation of Impact of Rejuvenators on Engineering Properties of RAP/RAS Mixes.

www.manaraa.com

Kandhal, P.S. and Mallick, R.B., 1998. Pavement Recycling Guidelines for State and Local Governments, Publications No. FHWA—SA —: 98-042.

Karki, P., 2010. Computational and experimental characterization of bituminous composites based on experimentally determined properties of constituents.

Karki, P., Kim, Y.-R. and Little, D.N., 2015. Dynamic Modulus Prediction of Asphalt Concrete Mixtures Through Computational Micromechanics, Transportation Research Board 94th Annual Meeting.

Kim, Y.-R. and Aragão, F.T.S., 2013. Microstructure modeling of rate-dependent fracture behavior in bituminous paving mixtures. Finite Elements in Analysis and Design, 63: 23-32.

Kim, Y.-R., Little, D. and Lytton, R., 2002. Use of dynamic mechanical analysis (dma) to evaluate the fatigue and healing potential of asphalt binders in sand asphalt mixtures (with discussion and closure). Journal of the Association of Asphalt Paving Technologists, 71.

Kim, Y.-R., Little, D. and Lytton, R., 2003a. Fatigue and healing characterization of asphalt mixtures. Journal of Materials in Civil Engineering, 15(1): 75-83.

Kim, Y.-R. and Little, D.N., 2005. Development of specification-type tests to assess the impact of fine aggregate and mineral filler on fatigue damage.

Kim, Y.-R., Little, D.N. and Song, I., 2003b. Mechanistic evaluation of mineral fillers on fatigue resistance and fundamental material characteristics. Transportation Research Board, Washington, DC.

www.manaraa.com

Kim, Y., Lee, H., Little, D. and Kim, Y.R., 2006. A Simple Testing Method to Evaluate Fatigue Fracture and Damage Performance of Asphalt Mixtures (With Discussion). Journal of the Association of Asphalt Paving Technologists, 75.

Lange, C. and Stroup-Gardiner, M., 2002. Characterization of asphalt odors and emissions, Ninth International Conference on Asphalt Pavements.

Lee, H.-J., 1996. Uniaxial constitutive modeling of asphalt concrete using viscoelasticity and continuum damage theory.

Li, R., Karki, P., Hao, P. and Bhasin, A., 2015. Rheological and low temperature properties of asphalt composites containing rock asphalts. Construction and Building Materials, 96: 47-54.

Mallick, R., Kandhal, P. and Bradbury, R., 2008. Using warm-mix asphalt technology to incorporate high percentage of reclaimed asphalt pavement material in asphalt mixtures. Transportation Research Record: Journal of the Transportation Research Board(2051): 71-79.

Menard, K.P., 2008. Dynamic mechanical analysis: a practical introduction. CRC press.

Mogawer, W. et al., 2012. Performance characteristics of plant produced high RAP mixtures. Road Materials and Pavement Design, 13(sup1): 183-208.

Mogawer, W.S., Austerman, A.J. and Bonaquist, R., 2009. Evaluating effects of warm-mix asphalt technology additive dosages on workability and durability of asphalt mixtures containing recycled asphalt pavement, Transportation research board 88th annual meeting.

www.manaraa.com

Mogawer, W.S., Booshehrian, A., Vahidi, S. and Austerman, A.J., 2013. Evaluating the effect of rejuvenators on the degree of blending and performance of high RAP, RAS, and RAP/RAS mixtures. Road Materials and Pavement Design, 14(sup2): 193-213.

Moghadas Nejad, F., Azarhoosh, A., Hamedi, G.H. and Roshani, H., 2014. Rutting performance prediction of warm mix asphalt containing reclaimed asphalt pavements. Road Materials and Pavement Design, 15(1): 207-219.

Palvadi, S., Bhasin, A. and Little, D., 2012. Method to quantify healing in asphalt composites by continuum damage approach. Transportation Research Record: Journal of the Transportation Research Board(2296): 86-96.

Reese, R., 1997. Properties of aged asphalt binder related to asphalt concrete fatigue life. Journal of the Association of Asphalt Paving Technologists, 66.

Shen, J., Amirkhanian, S. and Aune Miller, J., 2007a. Effects of rejuvenating agents on superpave mixtures containing reclaimed asphalt pavement. Journal of Materials in Civil Engineering, 19(5): 376-384.

Shen, J., Amirkhanian, S. and Tang, B., 2007b. Effects of rejuvenator on performance-based properties of rejuvenated asphalt binder and mixtures. Construction and Building Materials, 21(5): 958-964.

Shu, X., Huang, B., Shrum, E.D. and Jia, X., 2012. Laboratory evaluation of moisture susceptibility of foamed warm mix asphalt containing high percentages of RAP. Construction and Building Materials, 35: 125-130.

www.manaraa.com

Sondag, M.S., Chadbourn, B.A. and Drescher, A., 2002. Investigation of recycled asphalt pavement (RAP) mixtures.

Tao, M. and Mallick, R., 2009. Effects of warm-mix asphalt additives on workability and mechanical properties of reclaimed asphalt pavement material. Transportation Research Record: Journal of the Transportation Research Board(2126): 151-160.

Timm, D., Willis, J. and Kvasnak, A., 2011. Full-scale structural evaluation of fatigue characteristics in high reclaimed asphalt pavement and warm-mix asphalt. Transportation Research Record: Journal of the Transportation Research Board(2208): 56-63.

Tran, N.H., Taylor, A. and Willis, R., 2012. Effect of rejuvenator on performance properties of HMA mixtures with high RAP and RAS contents. Auburn, AL: National Center for Asphalt Technology.

Underwood, B.S. and Kim, Y.R., 2012. Microstructural Association Model for Upscaling Prediction of Asphalt Concrete Dynamic Modulus. Journal of Materials in Civil Engineering, 25(9): 1153-1161.

Underwood, B.S. and Kim, Y.R., 2013. Microstructural investigation of asphalt concrete for performing multiscale experimental studies. International Journal of Pavement Engineering, 14(5): 498-516.

Vasconcelos, K.L., Bhasin, A., Little, D.N. and Lytton, R.L., 2010. Experimental measurement of water diffusion through fine aggregate mixtures. Journal of Materials in Civil Engineering.

www.manaraa.com

Yu, X., Zaumanis, M., dos Santos, S. and Poulikakos, L.D., 2014. Rheological, microscopic, and chemical characterization of the rejuvenating effect on asphalt binders. Fuel, 135: 162-171.

Zaumanis, M., Mallick, R.B. and Frank, R., 2014. Evaluation of different recycling agents for restoring aged asphalt binder and performance of 100% recycled asphalt. Materials and Structures: 1-14.

Zhao, S., Huang, B., Shu, X., Jia, X. and Woods, M., 2012. Laboratory performance evaluation of warm-mix asphalt containing high percentages of reclaimed asphalt pavement. Transportation Research Record: Journal of the Transportation Research Board(2294): 98-105.

Zhao, S., Huang, B., Shu, X. and Woods, M., 2013. Comparative evaluation of warm mix asphalt containing high percentages of reclaimed asphalt pavement. Construction and Building Materials, 44: 92-100.

Zhou, F., Estakhri, C. and Scullion, T., 2014. Literature Review: Performance of RAP/RAS Mixes and New Direction.

www.manaraa.com